Lung Carcinoma

13

Chen Zhang and Jeffrey L. Myers

The classification and diagnostic criteria for lung carcinoma, the deadliest cancer in humans, undergo periodic updates. The 2015 World Health Organization (WHO) classification highlights changes in several categories of lung cancer, especially in the classification of adenocarcinomas and large cell carcinomas. For example, the clinically familiar term bronchioloalveolar carcinoma was discontinued and replaced with adenocarcinoma in situ and the related categories of minimally invasive and lepidic-predominant adenocarcinoma. Most of the tumors classified historically as mucinous bronchioloalveolar carcinomas are now considered invasive mucinous carcinomas. Basaloid carcinoma and large cell neuroendocrine carcinomas are separated as entities distinct from large cell carcinoma. In addition, immunophenotyping was introduced as an important criterion for phenotyping poorly differentiated non-small cell carcinomas, especially in small biopsies.

C. Zhang (✉)
Department of Pathology and Laboratory Medicine, Indiana University School of Medicine, Indianapolis, IN, USA
e-mail: chenzhan@iupui.edu

J. L. Myers
Department of Pathology, Michigan Medicine,
Ann Arbor, MI, USA
e-mail: myerjeff@med.umich.edu

Adenocarcinoma

Preinvasive (Atypical Adenomatous Hyperplasia and Adenocarcinoma In Situ)

Atypical Adenomatous Hyperplasia

Atypical adenomatous hyperplasia (Fig. 13.1) is a small (no more than 5 mm in greatest dimension), localized proliferation of mildly atypical type 2 pneumocytes and/or Clara cells distributed along alveolar septa without invasion. It is usually an incidental microscopic finding.
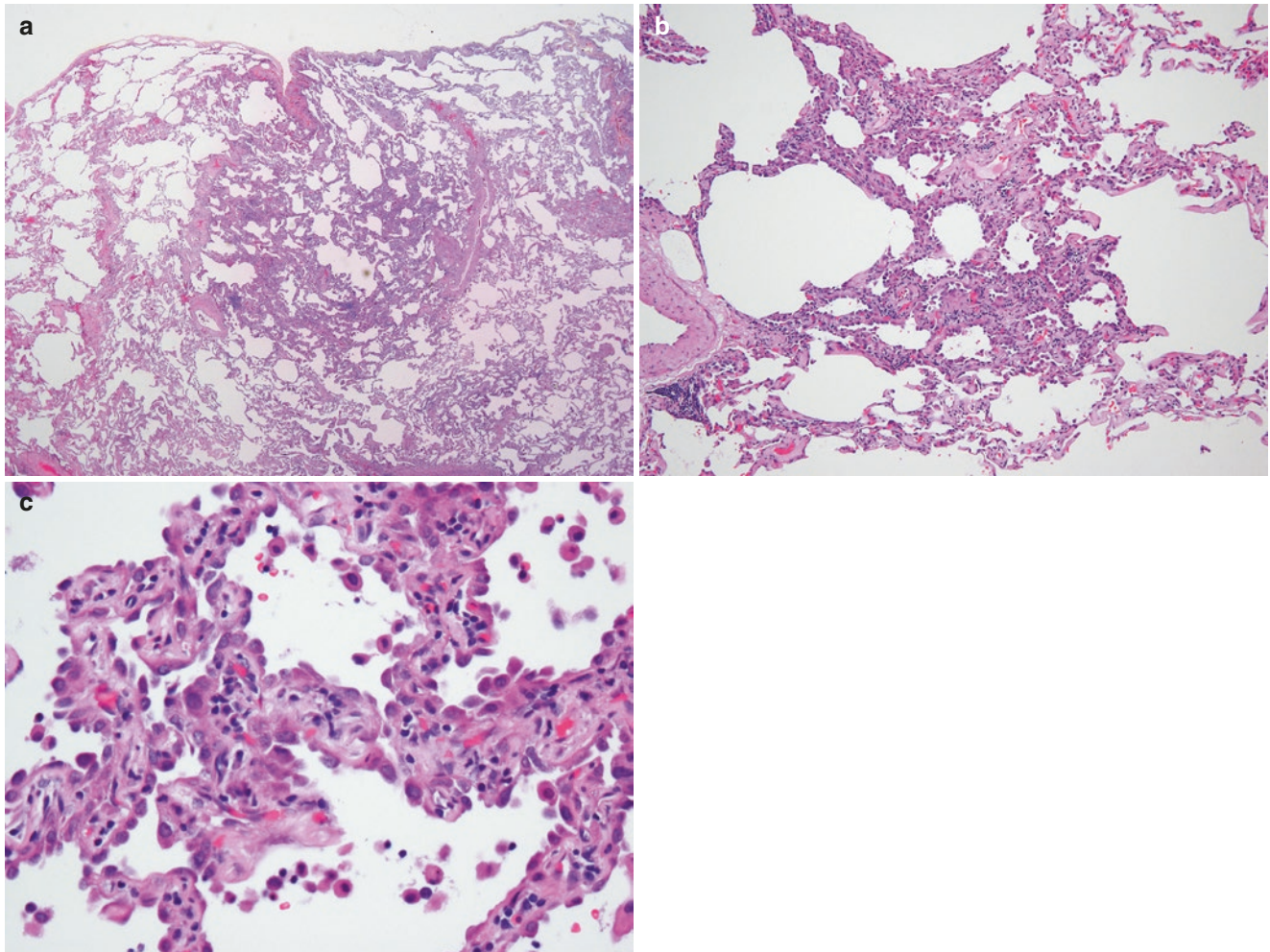
Fig. 13.1 Atypical adenomatous hyperplasia. (**a**) Low-magnification photomicrograph shows a small (2-mm) localized lesion. Compared to normal lung parenchyma, the lesion shows slightly thickened alveolar septa and atypical pneumocyte hyperplasia along the septa. The alveolar lung architecture is preserved, and there is no invasive component. (**b**) Higher magnification of area illustrated in **a** showing interface between atypical adenomatous hyperplasia (above) and normal lung (below). The former is characterized by thickening of alveolar septa and a proliferation of mildly atypical pneumocytes. (**c**) High-magnification view highlighting the atypical cells characterized by enlarged nuclei but with a very orderly single-cell layer without nuclear crowding or tufting. These atypical cells are positive for TTF-1 (not shown)

Adenocarcinoma In Situ

Adenocarcinoma in situ (Figs. 13.2, 13.3 and 13.4), formerly known as bronchioloalveolar carcinoma, is defined as a small (no more than 3 cm in greatest dimension) localized well-differentiated adenocarcinoma that grows along the pre-existing alveolar structure without invasion. There should also be no micropapillary component and/or detached tumor cells present away from the main tumor mass, a phenomenon referred to as spread through air spaces (STAS). Most adenocarcinomas in situ constitute nonmucinous columnar cells. Pure mucinous adenocarcinomas in situ without an invasive component are very rare.

Fig. 13.2 Adenocarcinoma in situ. Gross photograph shows a 2-cm, poorly defined tan nodular lesion beneath the pleura. These lesions are commonly described as ground-glass opacities on chest CT scan
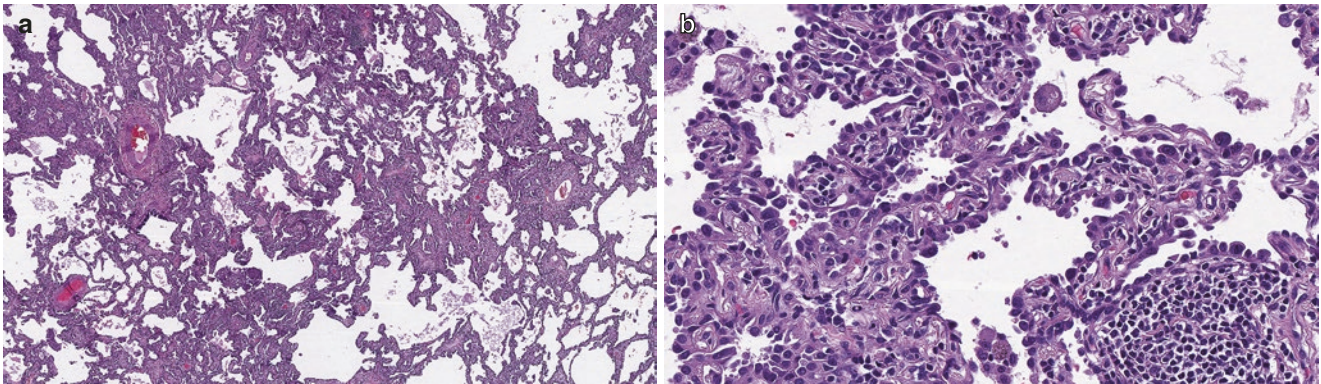
Fig. 13.3 Nonmucinous adenocarcinoma in situ. (**a**) Low-magnification photomicrograph shows a nonmucinous epithelial tumor growing along the preserved but thickened alveolar septa; no invasive foci are seen. (**b**) High-magnification view shows crowded tumor cells with hyperchromatic nuclei and occasional small nucleoli. Tumor cells grow along alveolar septa in a lepidic growth pattern without invasion
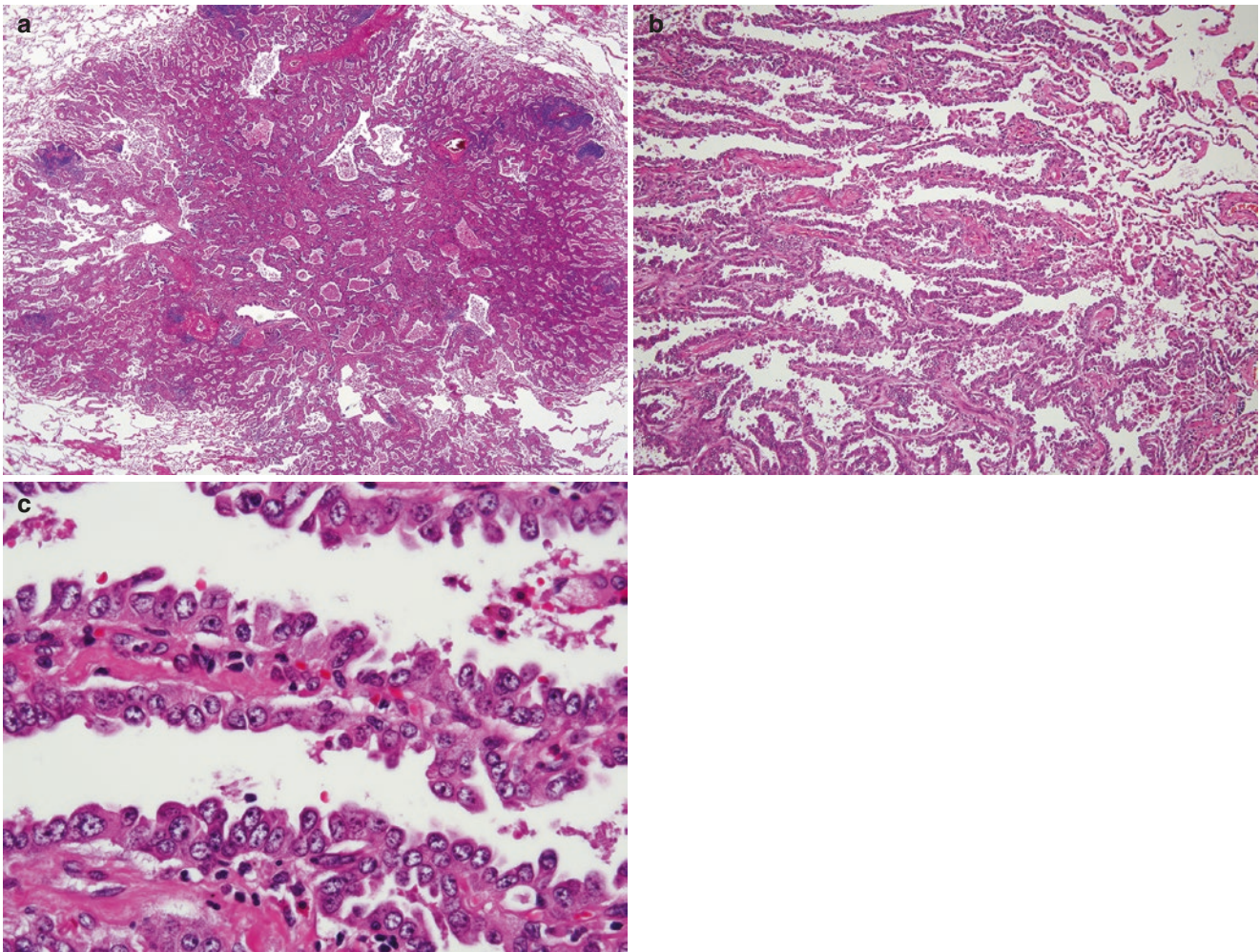
Fig. 13.4 Nonmucinous adenocarcinoma in situ. (**a**) Low-magnification view of another small (1.1 cm) adenocarcinoma in situ in which thickened but intact interstitial structures are lined by a population of atypical nonmucinous columnar cells. (**b**) Intermediate-magnification photomicrograph showing the interface between adenocarcinoma in situ and normal lung (right). (**c**) High-magnification view showing more rounded, cuboidal, and hobnail cells with a higher degree of cytologic atypia as evidenced by nuclear enlargement, aniso-nucleosis, and relatively scant cytoplasm

Minimally Invasive Adenocarcinoma

Minimally invasive adenocarcinoma (Figs. 13.5 and 13.6) is a small (no more than 3 cm in greatest dimension), solitary adenocarcinoma with a predominantly lepidic growth pattern and minimal invasion that measures no more than 5 mm in greatest dimension. The invasive component is most commonly an acinar subtype but can be any other subtype or variant. For all adenocarcinomas that have a prominent lepidic component comprising nonmucinous columnar cells, the current AJCC or *American Joint Committee on Cancer Staging Manual*, 8th edition, indicates that only the invasive component should be used for pT classification. Small (total gross tumors no more than 3 cm in greatest dimension) stage I adenocarcinomas in which a lepidic component consists of at least 50% of the cross-sectional area and in which there are no other histologic findings to suggest a more aggressive potential, such as angiolymphatic or visceral pleural invasion, a micropapillary component, spread through air spaces (STAS), and/or close parenchymal margins if less than lobectomy is performed, have the same excellent prognosis as adenocarcinoma in situ and minimally invasive adenocarcinomas.
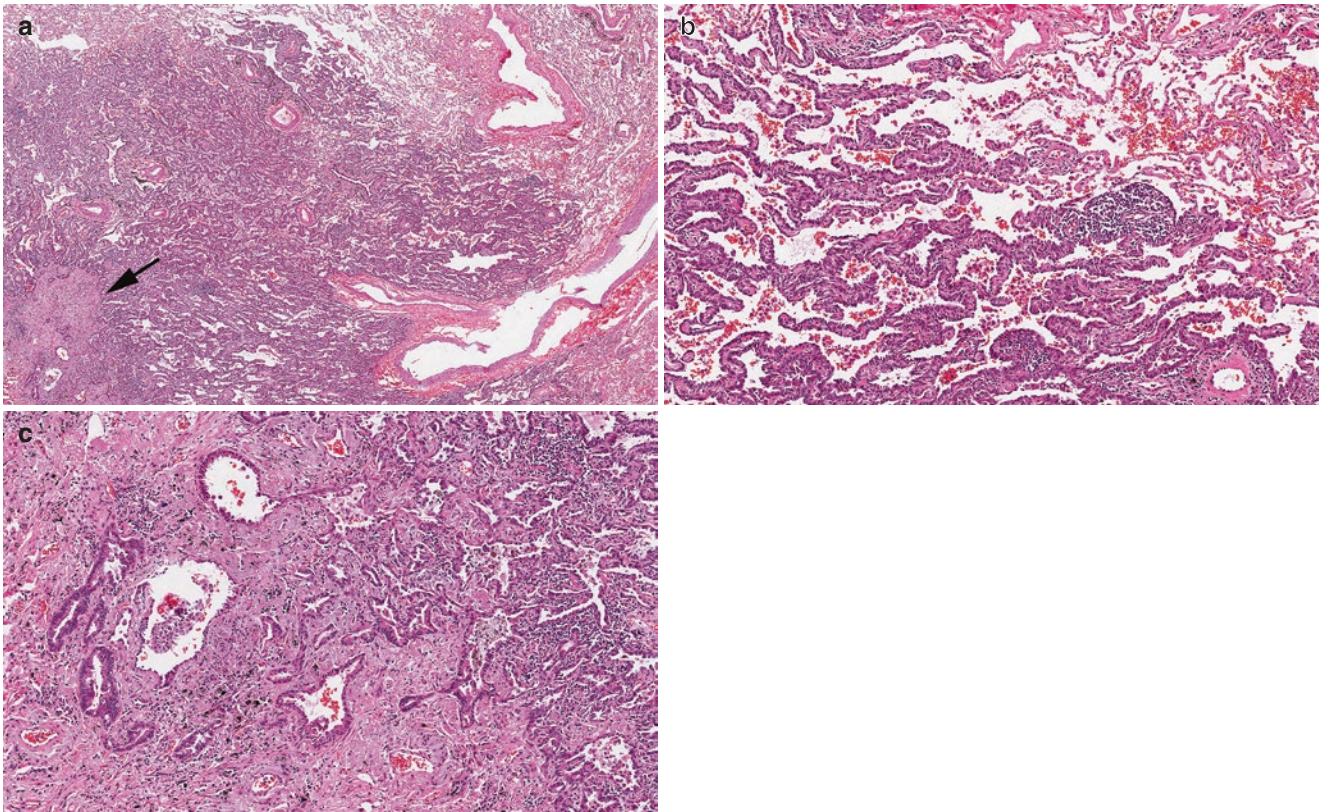
Fig. 13.5 Minimally invasive adenocarcinoma. (**a**) Low-magnification photomicrograph shows a small localized lesion (<3 cm) with a predominantly lepidic growth pattern and a small (<5 mm) focus of invasion (*arrow*). (**b**) Higher-magnification view of the noninvasive component in which tumor cells grow along intact alveolar septa in a lepidic pattern. (**c**) Photomicrograph showing the invasive component. The scarred area shows a small focus (<5 mm) of invasive adenocarcinoma, acinar type. The invasive component consists of small angulated glands inciting a myofibroblastic ("desmoplastic") stromal response. The tumor should be classified as a lepidic-predominant adenocarcinoma when the invasive component measures more than 5 mm
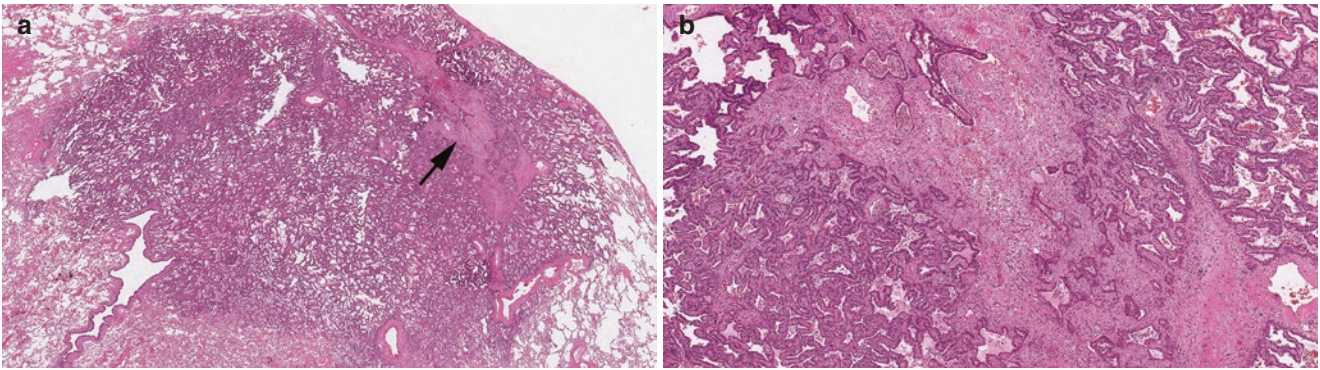
Fig. 13.6 Minimally invasive adenocarcinoma. (**a**) Low-magnification view of another example of a minimally invasive adenocarcinoma in which most of this small (just over 1 cm) peripheral, subpleural tumor has a lepidic growth pattern except for a small area of invasion in an area of scarring (*arrow*). (**b**) Photomicrograph showing the invasive component that measures only 4 mm and demonstrates features similar to those illustrated and described in Fig. 13.5c

Invasive Adenocarcinoma

Invasive adenocarcinoma (Figs. 13.7, 13.8, 13.9, 13.10, 13.11, 13.12, 13.13, 13.14, 13.15, 13.16 and 13.17) is a malignant epithelial tumor with glandular differentiation, mucin production, and/or immunohistochemical stains showing pneumocyte marker expression (i.e., TTF-1 and/or napsin A). In the 2015 WHO classification for resected tumors (*The 2015 World Health Organization Classification of Lung Tumors*), invasive adenocarcinomas are classified according to the predominant growth pattern or as a specific variant (Table 13.1). While the WHO recommends cataloguing all growth patterns identified in an adenocarcinoma in 5% increments, there is no proven clinical usefulness to this practice. Selecting the predominant pattern can be helpful in separating invasive adenocarcinomas into prognostically useful subsets as summarized in Table 13.2.
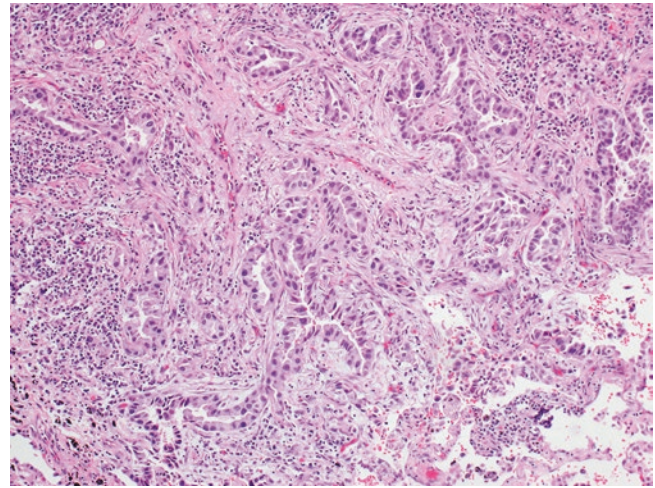
Fig. 13.7 Acinar adenocarcinoma. Photomicrograph showing a tumor composed of irregularly shaped glands with central luminal spaces invading a myofibroblastic stroma. Nuclei are enlarged and hyperchromatic, with anisonucleosis and occasionally prominent nucleoli
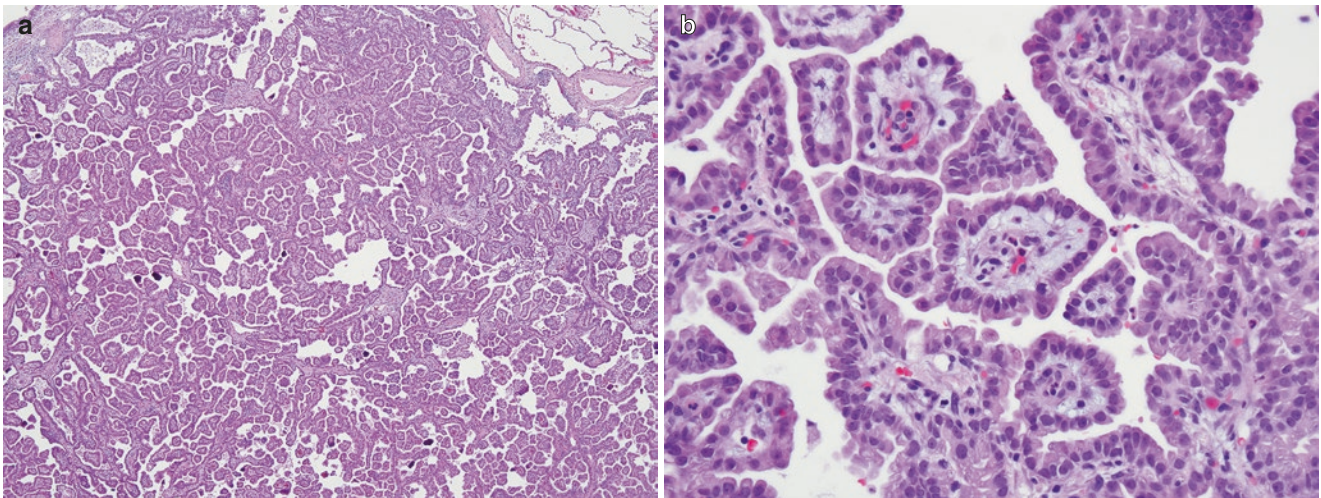
Fig. 13.8 Papillary adenocarcinoma. (**a**) Photomicrograph shows a tumor in which malignant columnar cells are growing on the surface of fibrovascular cores. (**b**) Higher-magnification view reveals cuboidal to columnar tumor cells growing on the surface of a true fibrovascular core
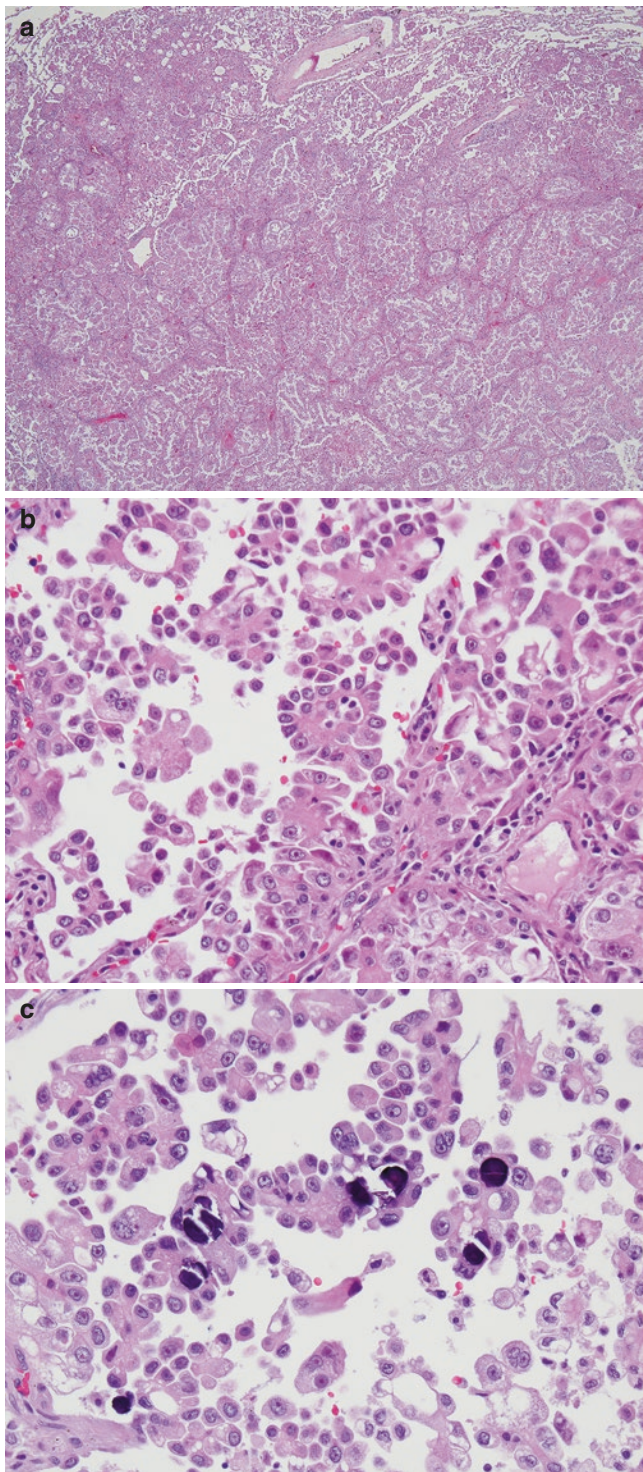
Fig. 13.9 Micropapillary adenocarcinoma. (**a**) Low-magnification photomicrograph shows tumor cells growing in numerous papillary tufts detached from or connected to alveolar walls. (**b**) High-magnification view shows tumor cells forming tufts and florets without a fibrovascular core. (**c**) Another high-magnification view shows detached small tumor aggregates with psammoma bodies floating in the alveolar air space. Tumor cells in this field show a higher degree of cytologic atypia
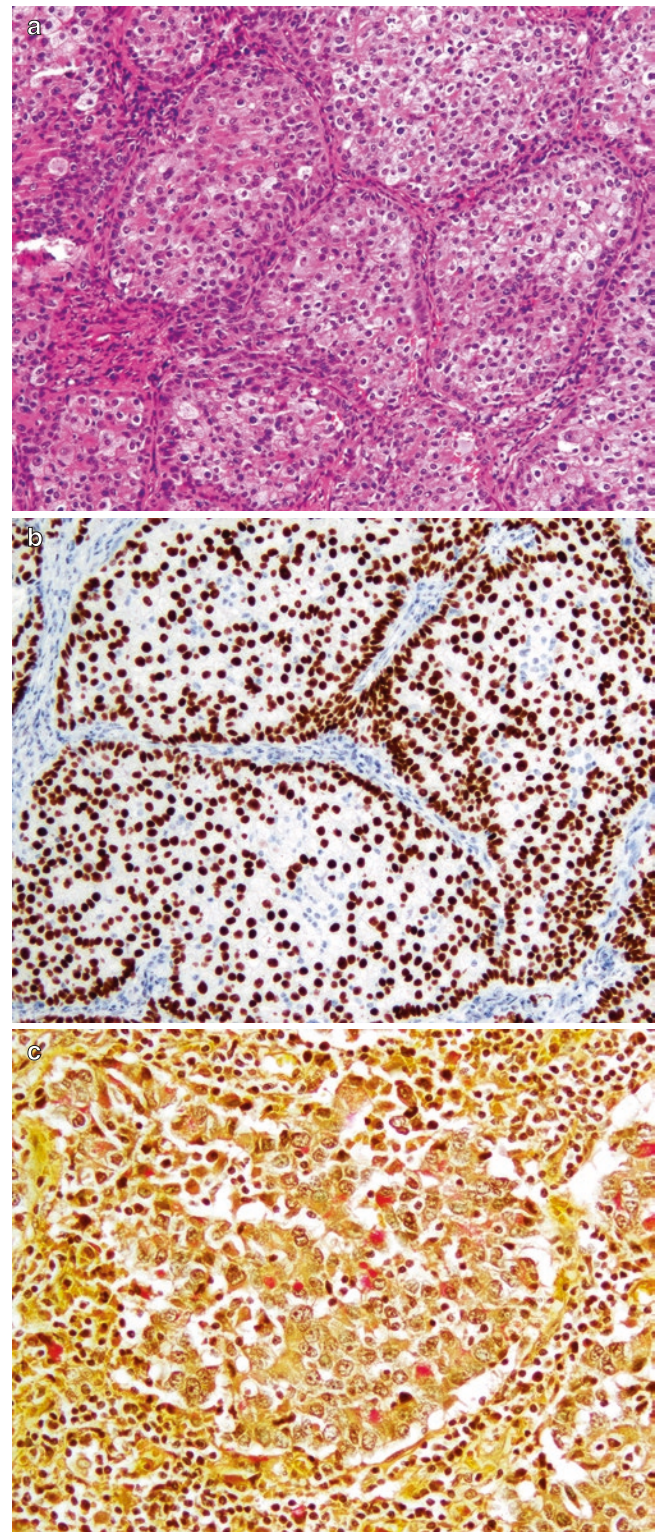
Fig. 13.10 Solid adenocarcinoma. (**a**) Photomicrograph showing tumor cells arranged as solid nests with abundant pale-staining eosinophilic to clear cytoplasm resembling squamous cell carcinoma. (**b**) Higher-magnification photomicrograph of an immunohistochemical-stained section shows strong positivity for TTF-1 in tumor cells. (**c**) Photomicrograph showing a mucicarmine stain that highlights intracellular mucin in occasional tumor cells
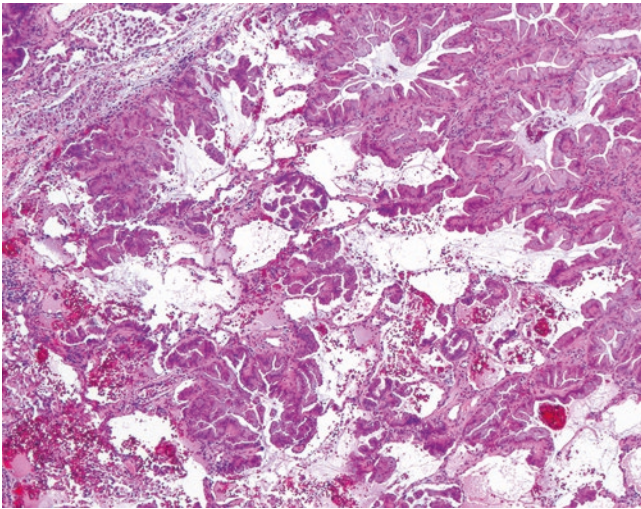
Fig. 13.11 Invasive mucinous adenocarcinoma. Low-magnification photomicrograph showing columnar neoplastic cells with abundant apical cytoplasmic mucin and basally oriented nuclei. This area shows both lepidic and papillary growth patterns, with variably conspicuous extracellular mucin
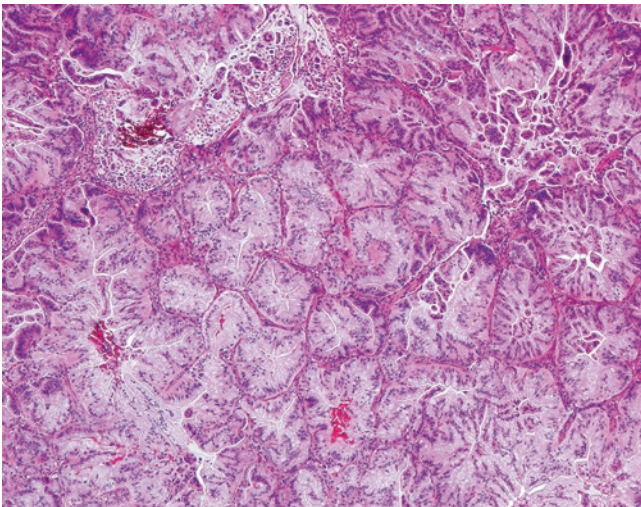
Fig. 13.12 Invasive mucinous adenocarcinoma. Photomicrograph showing a mucinous adenocarcinoma in which columnar mucinous cells are arranged in an acinar growth pattern characterized by closely packed, back-to-back glands separated by thin fibrotic septa. Foci of micropapillary growth are also present
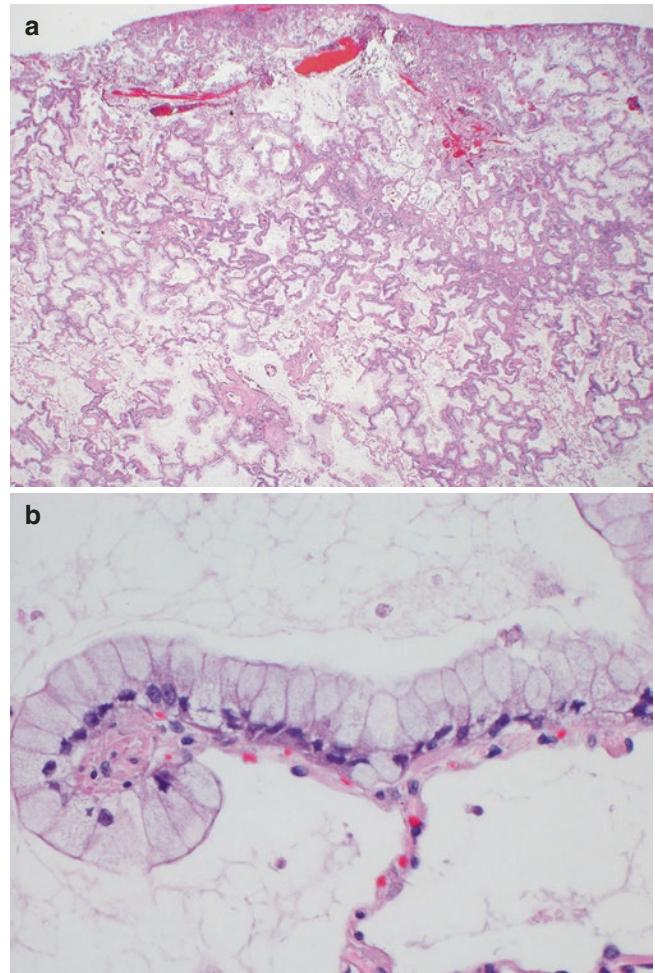
Fig. 13.13 Invasive mucinous adenocarcinoma. (**a**) Low-magnification photomicrograph of another example of invasive mucinous adenocarcinoma with a predominantly lepidic growth pattern. (**b**) High-magnification photomicrograph showing the remarkably bland cytologic features in neoplastic cells distributed along alveolar septa with small basally oriented nuclei and abundant apical mucin
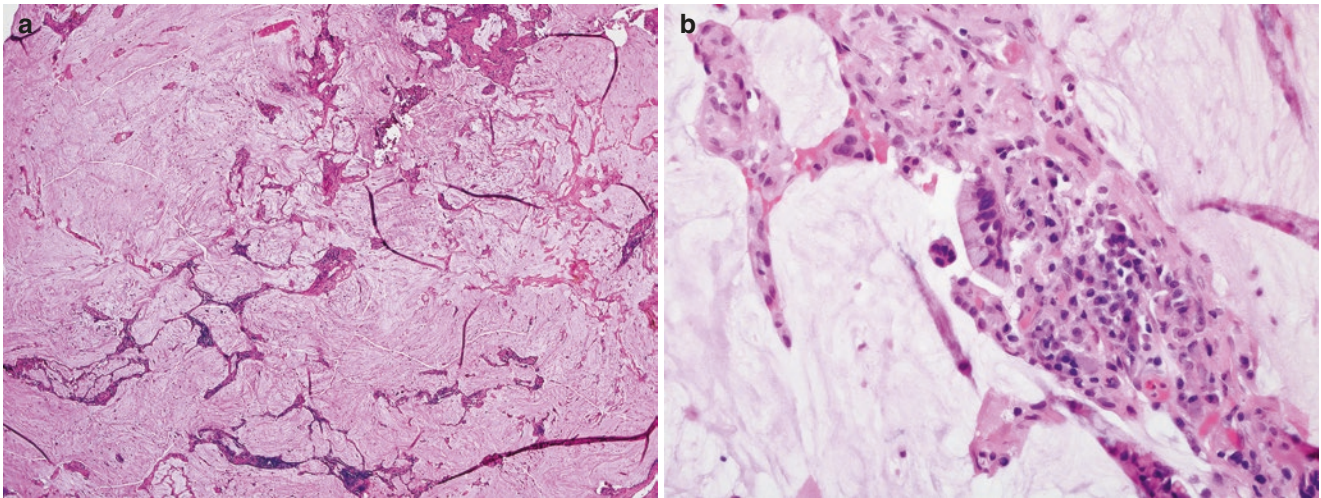
Fig. 13.14 Colloid adenocarcinoma. (**a**) Low-magnification photomicrograph showing a tumor characterized by pools of paucicellular pale-staining mucin, distending air spaces, and dissecting interstitial connective tissue. Tumor cells are rare and may be remarkably bland.

(**b**) High-magnification view showing rare well-differentiated mucinous glandular epithelium growing along the fibrous septa and floating in pools of extracellular mucin
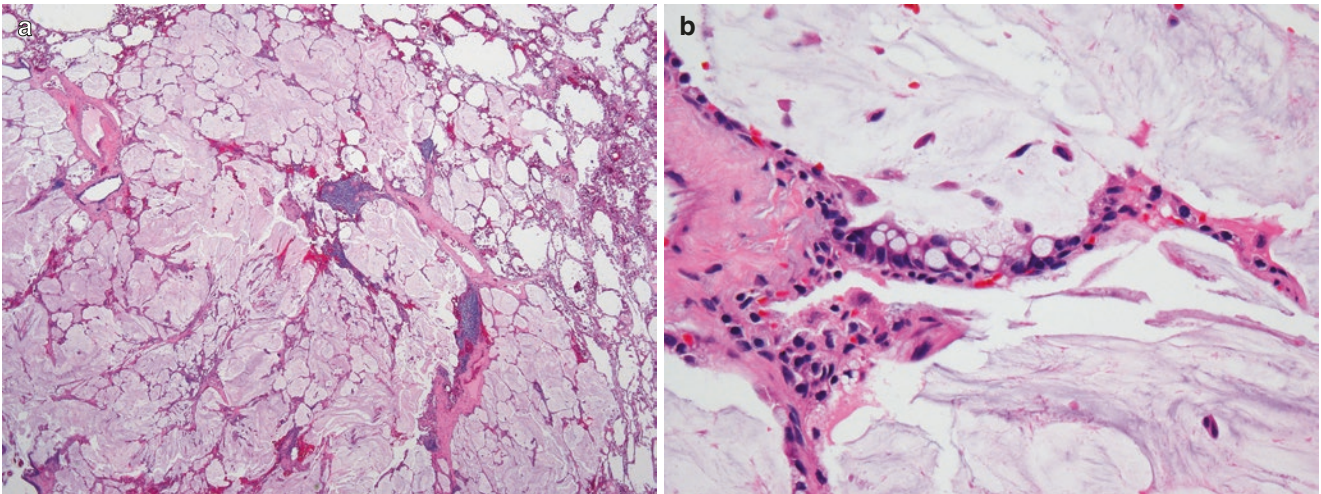
Fig. 13.15 Colloid adenocarcinoma. (**a**) Low-magnification photomicrograph showing another example of colloid adenocarcinoma in which large pools of paucicellular extracellular mucin distend air spaces. (**b**)

High-magnification photomicrograph showing isolated clusters of neoplastic epithelium resembling intestinal epithelium with goblet cells
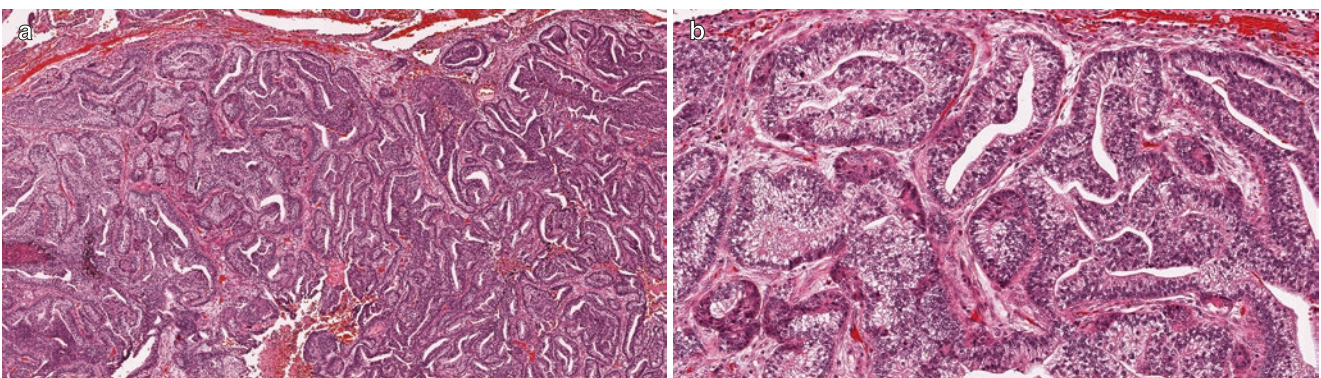
Fig. 13.16 Fetal adenocarcinoma. (**a**) Low-magnification photomicrograph showing an adenocarcinoma with a well-developed glandular growth pattern resembling fetal lungs with well-differentiated endometri-

oid adenocarcinomas. (**b**) High-magnification view showing columnar tumor cells with cytoplasmic glycogen vacuoles and nuclear stratification, furthering the resemblance to endometrioid adenocarcinoma
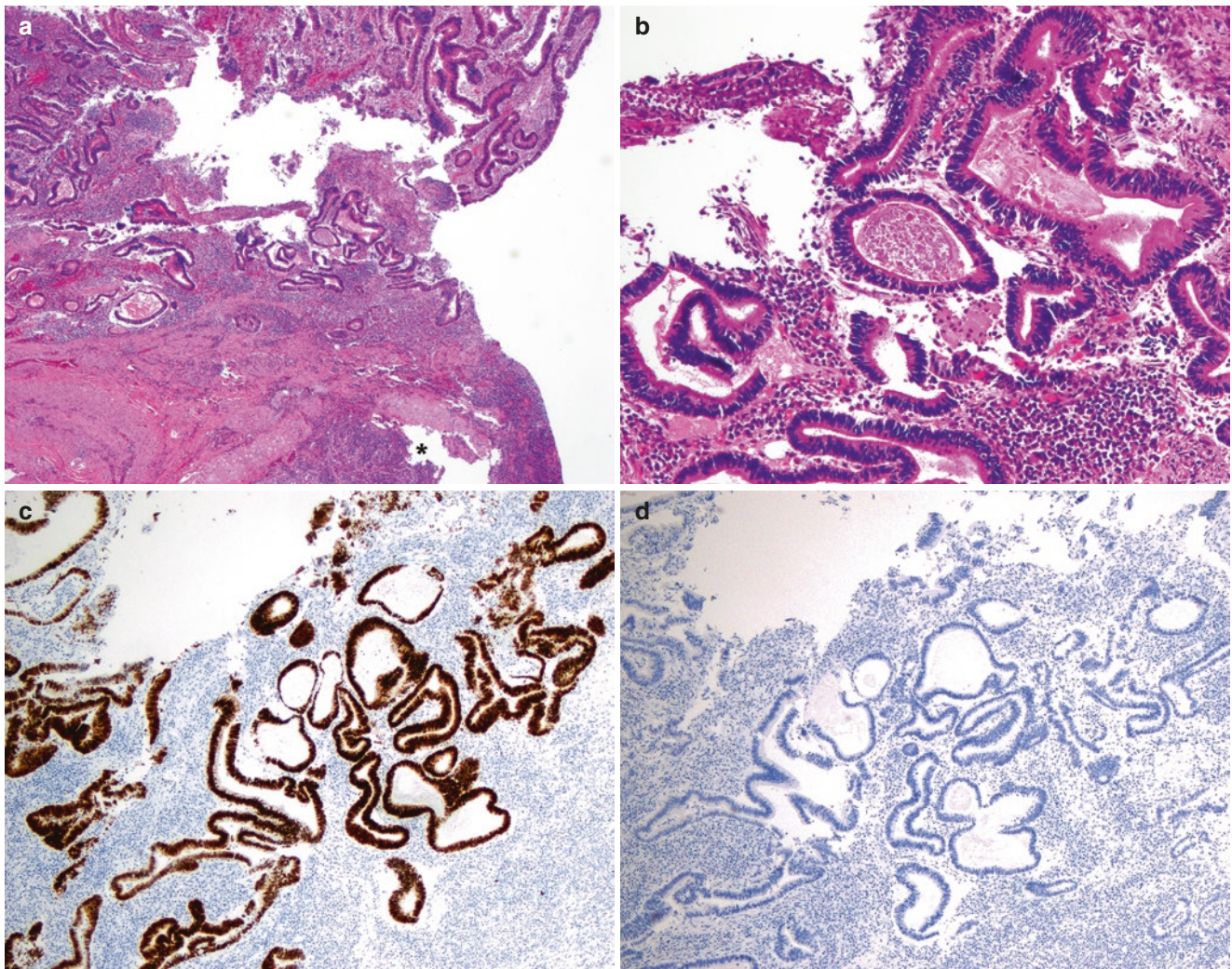
Fig. 13.17 Enteric adenocarcinoma. (**a**) Low-magnification photomicrograph shows an adenocarcinoma with well-formed glands and abundant inflammatory infiltrates next to a cartilaginous airway (*). (**b**) High-magnification view showing the tall, columnar stratified tumor cells forming glands with luminal necrosis. The morphologic features and immunoprofile are indistinguishable from those of colorectal adenocarcinoma. A clinical history and radiologic information are required to differentiate these two entities. (**c**) and (**d**), Immunohistochemical-stained sections showing strong, diffuse staining for CDX-2 (**c**) and negative staining for TTF-1 (**d**) in enteric adenocarcinoma

Table 13.1 Histologic subtypes and variants of adenocarcinoma

Subtypes (predominant growth pattern)	Lepidic
	Acinar
	Papillary
	Micropapillary
	Solid
Variants	Invasive mucinous adenocarcinoma
	Colloid adenocarcinoma
	Fetal adenocarcinoma
	Enteric adenocarcinoma

Table 13.2 Grading lung adenocarcinomas predominantly using histology

Grade	Predominant growth pattern/variant
Low grade/well differentiated	Adenocarcinoma in situ Minimally invasive adenocarcinoma Lepidic-predominant adenocarcinoma
Intermediate grade/moderately differentiated	Acinar Papillary Invasive mucinous
High grade/poorly differentiated	Solid Micropapillary

Squamous Cell Carcinoma

Squamous cell carcinoma in situ (Fig. 13.18) is a precursor lesion of invasive squamous cell carcinoma, arising in the bronchial epithelium of large airways
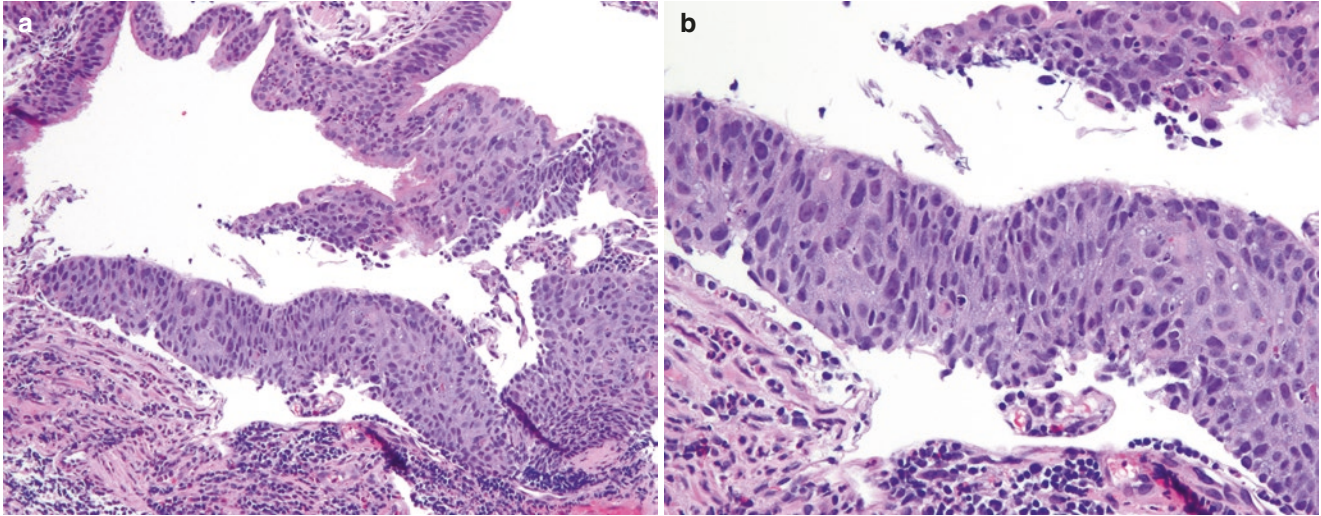
Fig. 13.18 Squamous cell carcinoma in situ. (**a**) Low-magnification photomicrograph showing squamous cell carcinoma in situ arising in a large respiratory airway with concomitant squamous metaplasia. (**b**) High-magnification photomicrograph showing dysplastic squamous cells with enlarged hyperchromatic nuclei, prominent nucleoli, mitotic figures above the basal cell layer, and anisonucleosis in the context of a disordered architecture extending from the base to the surface of the epithelium

Invasive Squamous Cell Carcinoma

Invasive squamous cell carcinoma (Figs. 13.19, 13.20 and 13.21) is defined as a malignant epithelial tumor that shows keratinization and/or intercellular bridges or a mor-phologically undifferentiated non-small cell carcinoma that expresses squamous cell markers (i.e., p63, p40, and/or high molecular weight cytokeratins for which CK5/6 has much higher specificity than 34βE12). It is negative for TTF-1.
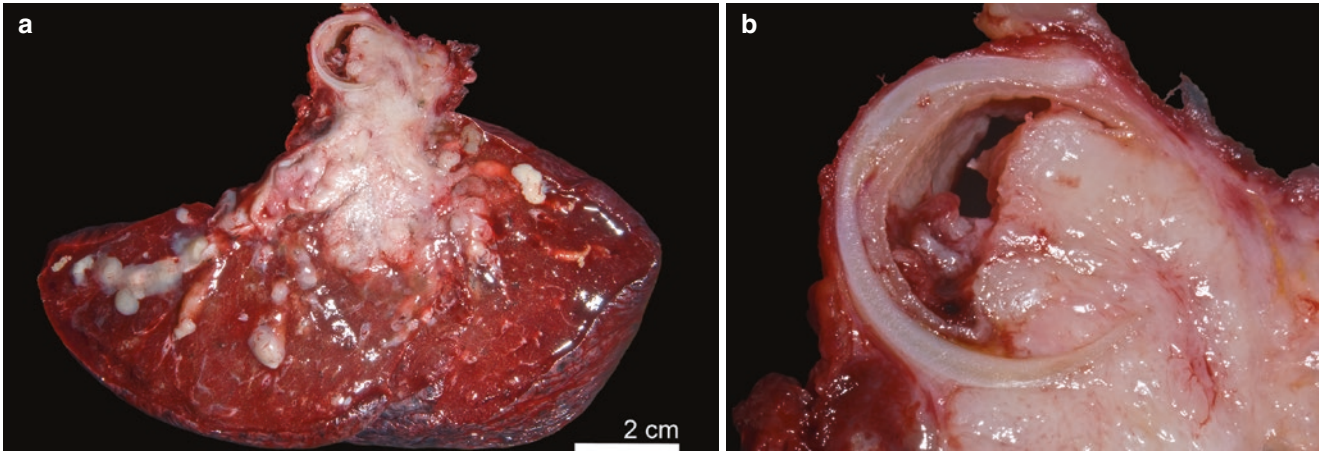
Fig. 13.19 Squamous cell carcinoma. (**a**) Gross photograph showing a centrally located obstructing mass extensively involving a large bronchus and surrounding lung parenchyma, with post-obstructive bronchi-ectasis in which dilated airways are filled with mucus. (Courtesy of J. Carvalho, Minneapolis, MN). (**b**) Closer view of the endobronchial mass. (Courtesy of J. Carvalho, Minneapolis, MN)
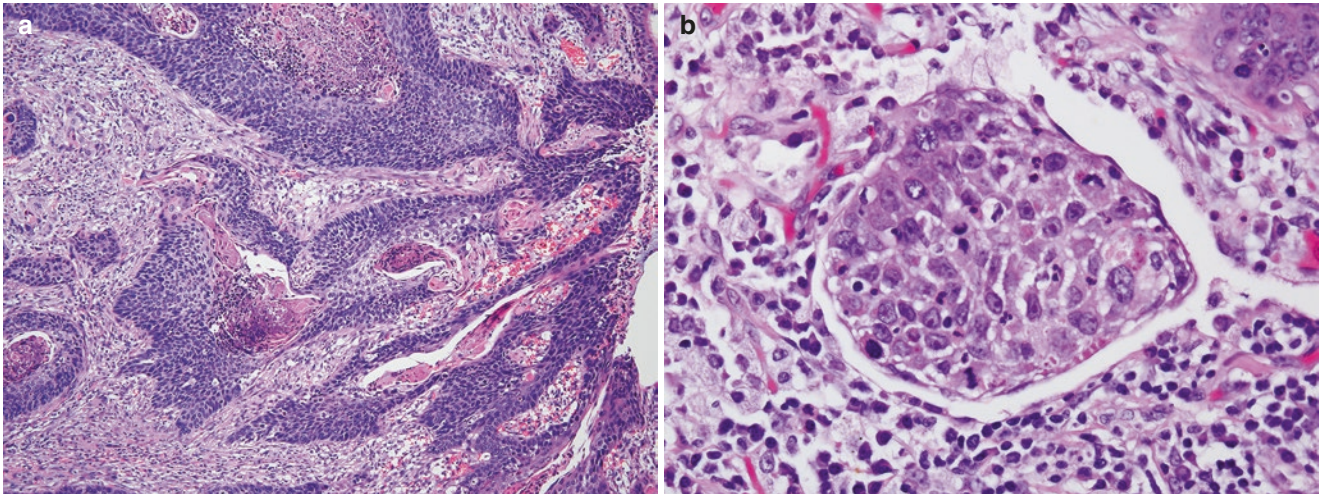
Fig. 13.20 Keratinizing squamous cell carcinoma. (**a**) Photomicrograph showing infiltrating nests with central keratinization in a desmoplastic stroma. (**b**) High-magnification photomicrograph showing another squamous cell carcinoma in which there are prominent intercellular bridges
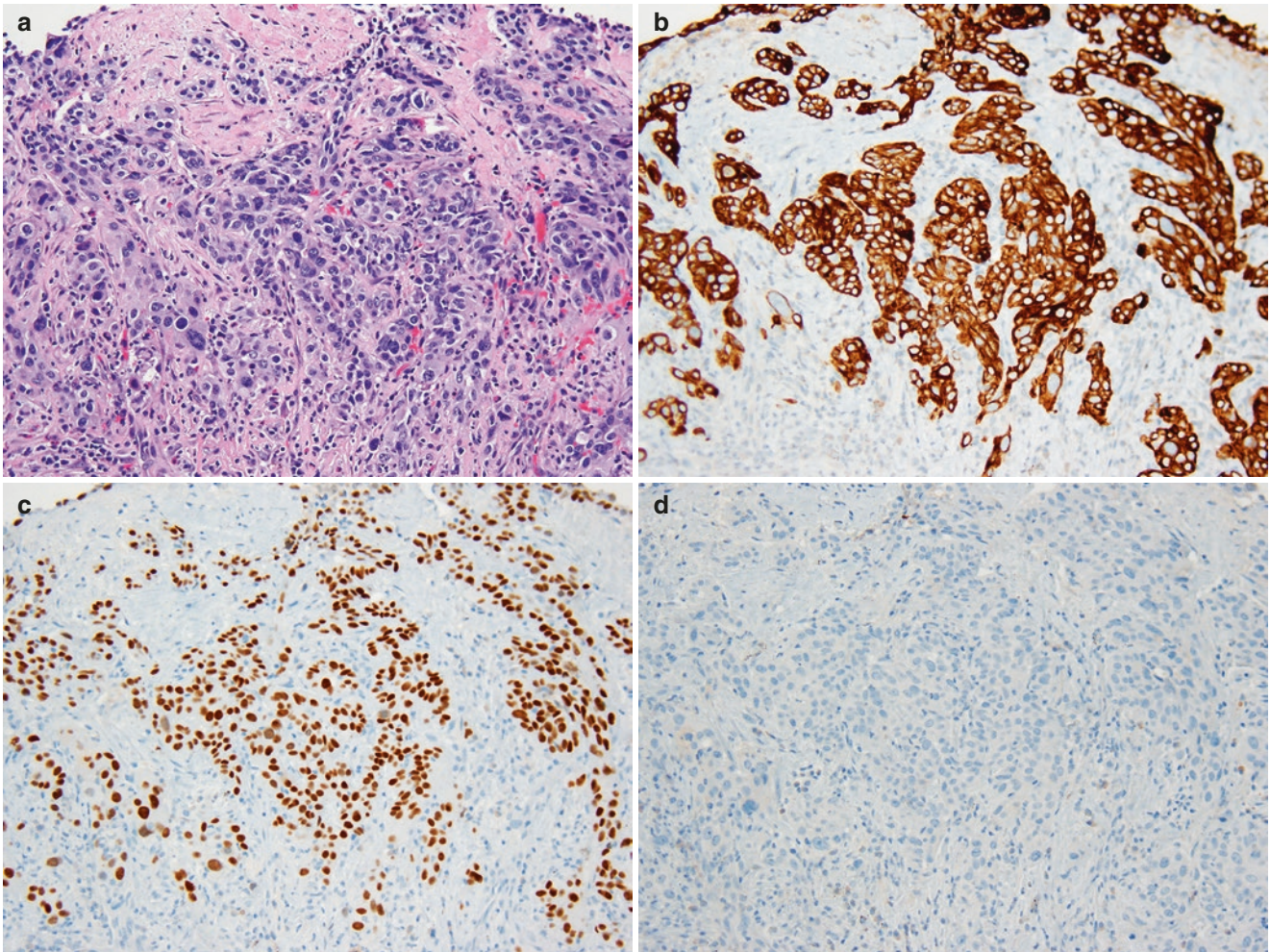
Fig. 13.21 Nonkeratinizing squamous cell carcinoma. (**a**) High-magnification photomicrograph showing poorly differentiated squamous cell carcinoma constituting infiltrating tumor cells with abundant cytoplasm but without easily identifiable intercellular bridging or keratinization. It is the sort of carcinoma that might be difficult to recognize as squamous based on routine histology alone. (**b–d**) Photomicrographs showing strong diffuse staining for high molecular weight cytokeratins (CK5/6) (**b**) and p63 (**c**) with negative staining for TTF-1 (**d**)

Basaloid Squamous Cell Carcinoma

Basaloid squamous cell carcinoma (Fig. 13.22) is a poorly differentiated malignant epithelial tumor composed of small cells arranged in large nests with a lobular architecture and peripheral palisading. The tumor cells lack squamous morphology but express squamous immunohistochemical markers such as p63 and p40. This tumor was previously considered a variant of large cell carcinoma but was recognized as a variant of squamous cell carcinoma in the 2015 WHO classification. Histologically, heterogeneous tumors with a component of conventional squamous cell carcinoma and a basaloid component that accounts for over 50% of the sample tumor are also classified as basaloid squamous cell carcinomas. These high-grade tumors tend to be associated with a prognosis that is poorer than that of other non-small cell carcinomas at the same stage.
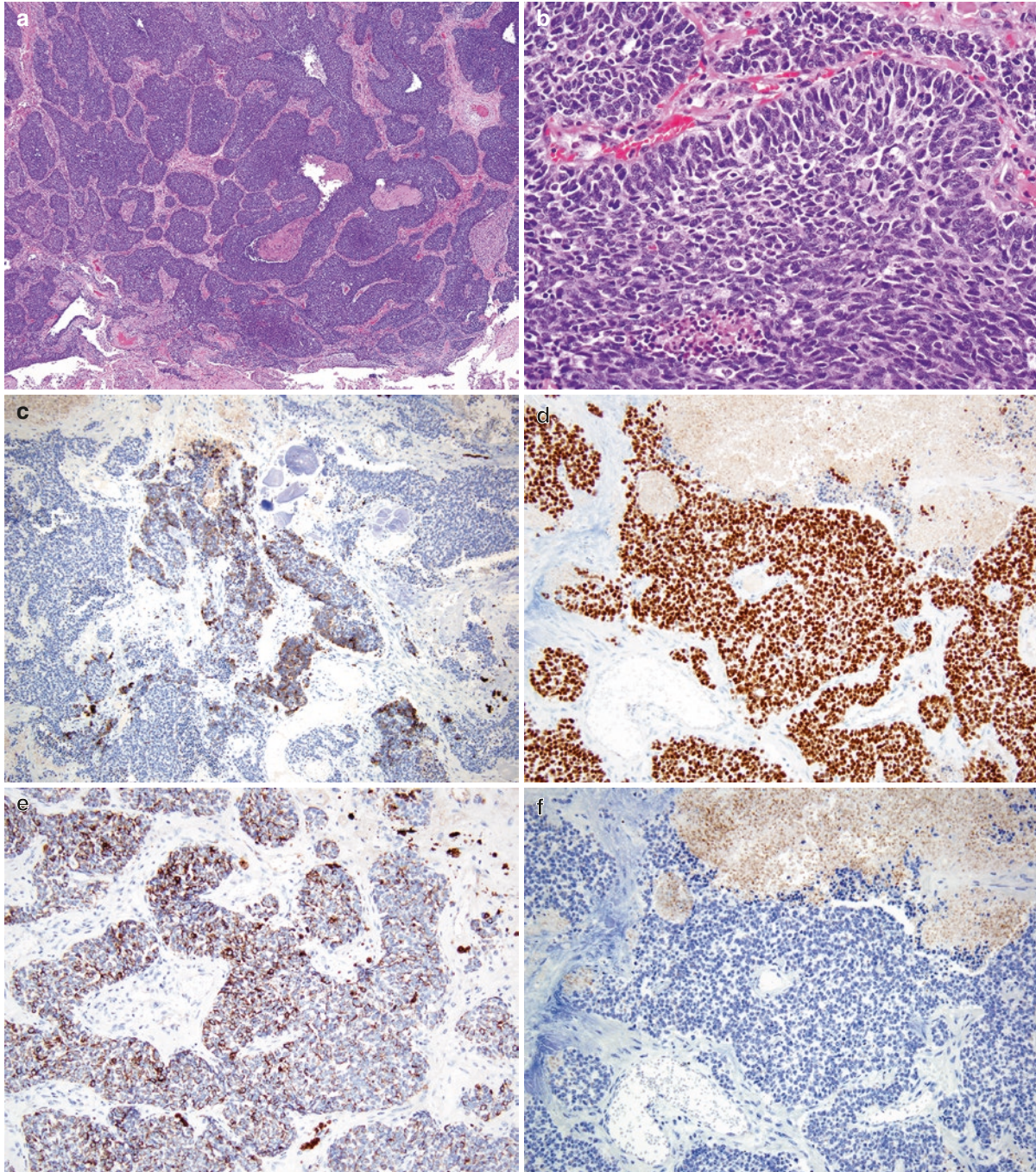
Fig. 13.22 Basaloid squamous cell carcinoma. (**a**) Low-magnification photomicrograph of basaloid squamous cell carcinoma shows solid, anastomosing nests with peripheral palisading and central comedo-type necrosis. (**b**) High-magnification view showing tumor cells that lack keratinization and intercellular bridges but demonstrate peripheral palisading and comedo-type necrosis. The tumor cells are relatively small and monomorphic, with hyperchromatic finely granular chromatin resembling small cell carcinoma. (**c**) As illustrated in this photomicrograph, the tumor may show focal and generally weak staining for synaptophysin, which may further confound the differential diagnosis with small cell carcinoma. However, positive staining for p63 (**d**) and CK5/6 (**e**) with negative staining for TTF-1 (**f**) can be extremely helpful, especially on small biopsies

Adenosquamous Carcinoma

Adenosquamous carcinoma (Fig. 13.23) is a carcinoma with components of both squamous cell carcinoma and adenocarcinoma, with each component constituting at least 10% of the tumor.
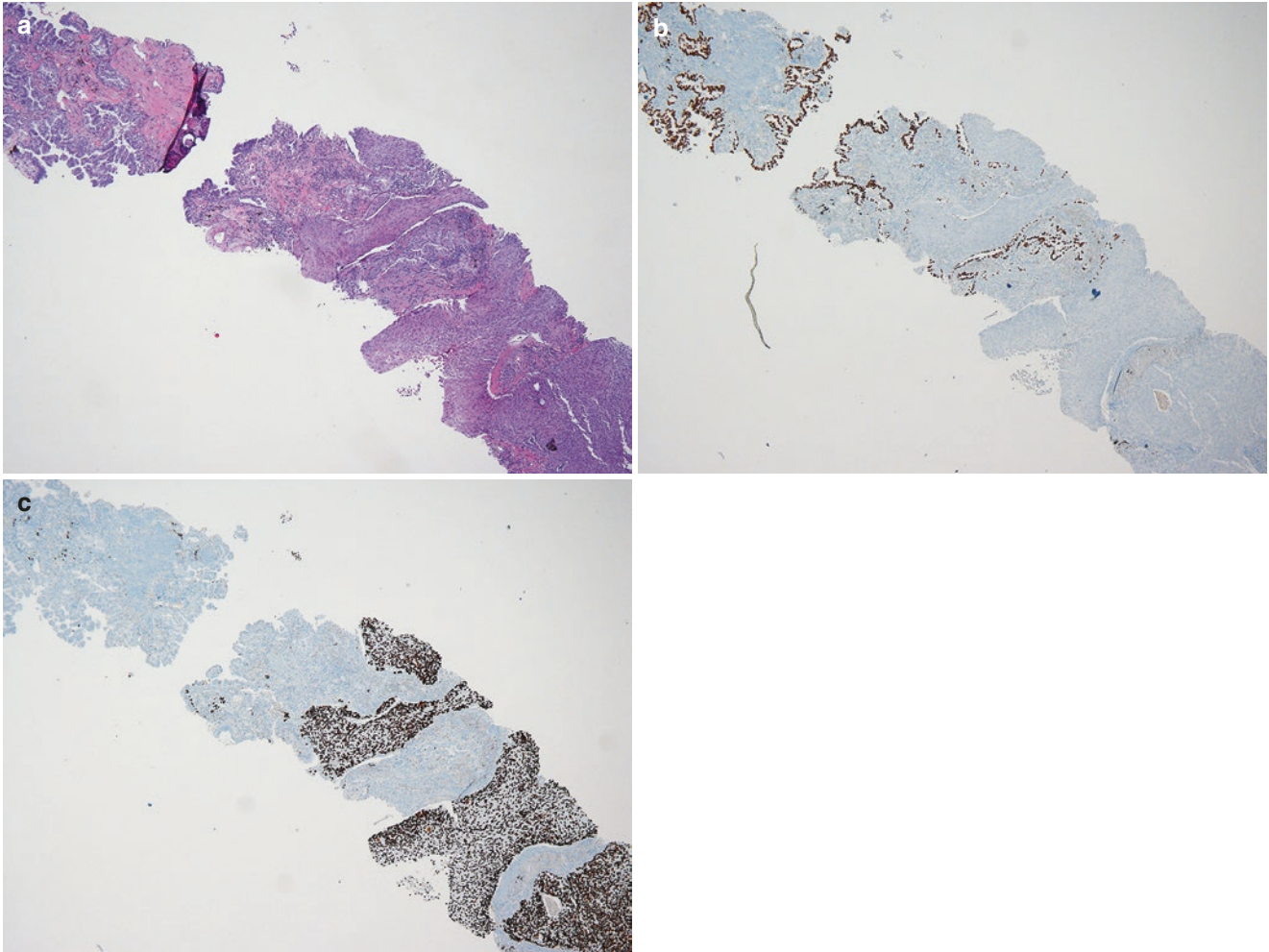
Fig. 13.23 Adenosquamous carcinoma. (**a**) Photomicrograph of core needle biopsy from a lung tumor showing both adenocarcinoma (upper left) and squamous cell carcinoma (lower right). (**b**) and (**c**), An immunohistochemical stain for TTF-1 highlights the adenocarcinoma component on the left (**b**), while p63 strongly and diffusely stains the squamous cell component on the right (**c**)

Neuroendocrine Tumors

Carcinoid Tumors

Carcinoid tumors (Figs. 13.24, 13.25, 13.26, 13.27, 13.28, 13.29, 13.30 and 13.31) are low- to intermediate-grade neuroendocrine malignancies that are divided into two subcategories: typical and atypical carcinoid tumors. Typical carcinoid tumors are the exemplars of neuroendocrine neoplasms in the lung and as such are distinguished by the same combination of growth patterns that characterize neuroendocrine neoplasms at other sites (Table 13.3). Typical carcinoid tumors consist of bland cuboidal and occasionally spindled cells with only modest degrees of anisonucleosis and with finely divided chromatin, small nucleoli, and variably abundant cytoplasm. Mitoses and tumor necrosis are not present, although endobronchial tumors may show surface ulceration with the anticipated degree of ulcer-related necrosis. Carcinoid tumors should measure at least 5 mm in greatest dimension to distinguish them from carcinoid tumorlets that are typically less than 5 mm in size and almost invariably are poorly circumscribed and intimately associated with bronchiolar epithelium.

Atypical carcinoid tumors are separated from typical carcinoid tumors based on a combination of necrosis and/or mitotic rate (Table 13.4). The Ki-67 labeling index correlates with histologic subclassification but does not improve on the prognostic value of the WHO classification criteria. Atypical carcinoid tumors overlap at the extreme with large cell neuroendocrine carcinoma but have lower mitotic rates ($\leq 10/2$ mm^2).
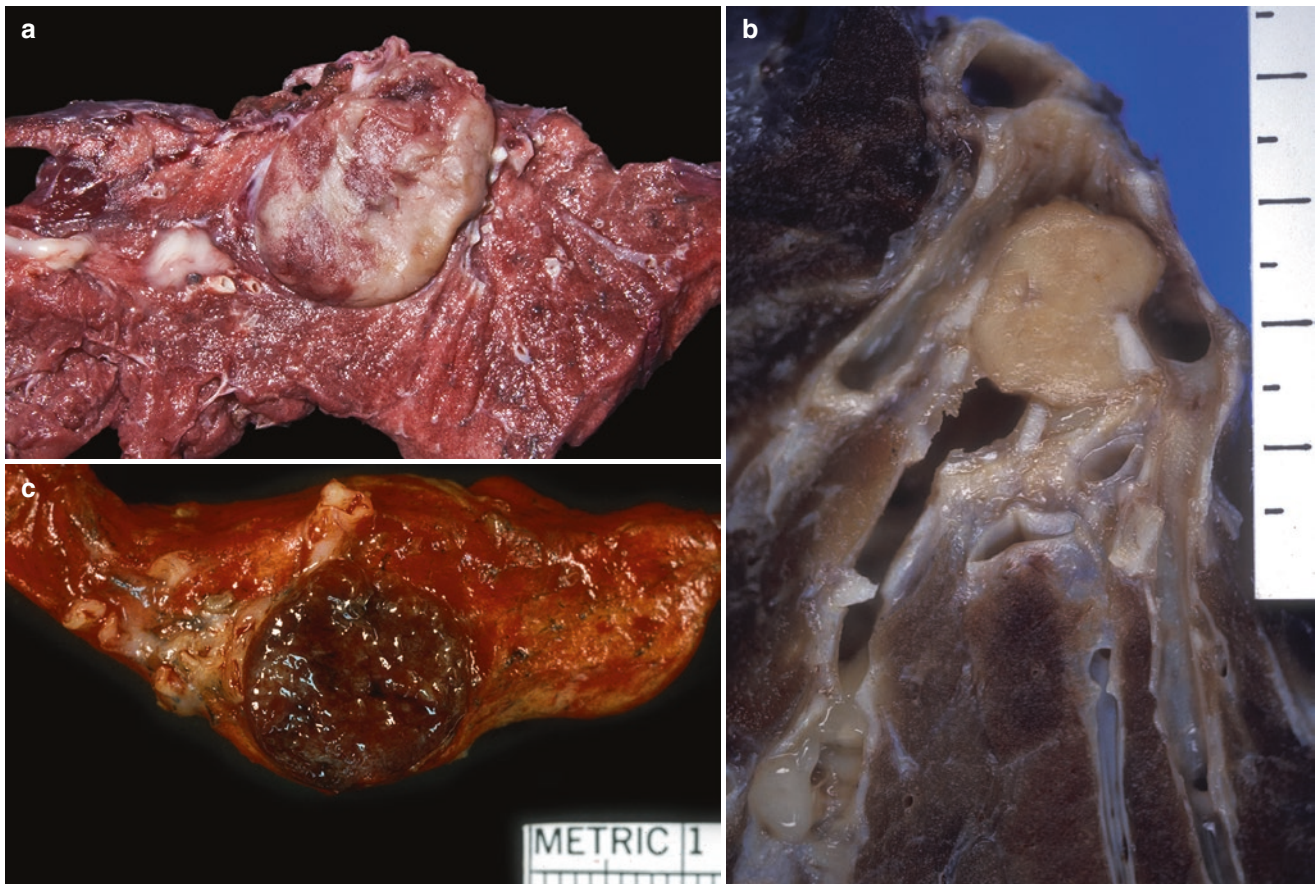
Fig. 13.24 Carcinoid tumor. (**a**) Gross photograph of a centrally located well-circumscribed tan-brown mass, partially obstructing the bronchus with post-obstructive mucus plugging on the left. (Courtesy of J. Carvalho, Minneapolis, MN). (**b**) Photograph showing cut surface of another centrally situated endobronchial carcinoid tumor. About three fourths of carcinoid tumors present as endobronchial masses. (**c**) Gross photograph of a peripheral carcinoid tumor with a deep mahogany color
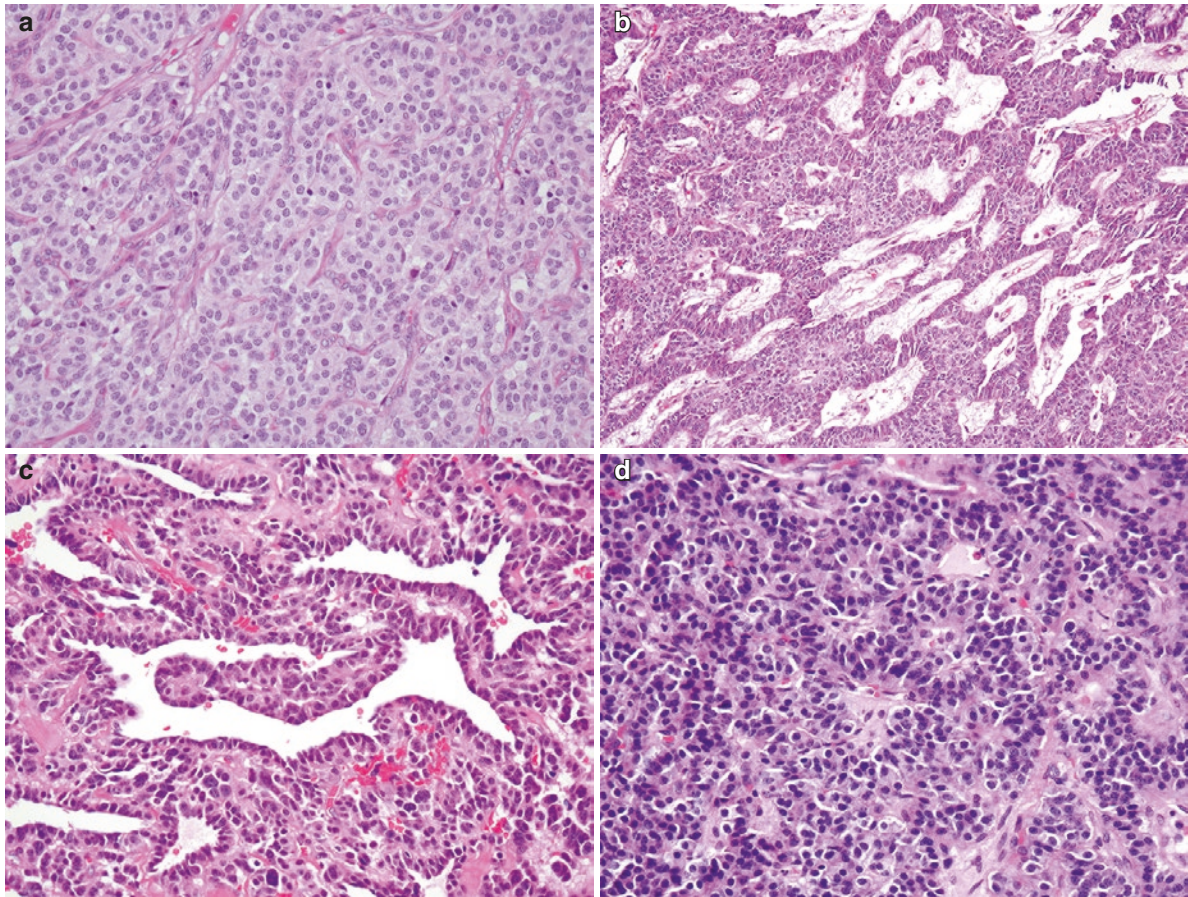
Fig. 13.25 Typical carcinoid tumor. (**a**) Photomicrograph showing tumor composed of bland cuboidal cells with a moderate amount of pale eosinophilic cytoplasm and finely granular chromatin. The cells are arranged in an organoid nesting pattern with delicate vascular stroma. No mitosis or necrosis is seen. (**b**) Photomicrograph showing trabecular pattern in a typical carcinoid tumor. Prominent edematous and pale-staining stroma are present between the trabecular bands of tumor cells. (**c**) Photomicrograph showing pseudoglandular and papillary patterns in a typical carcinoid tumor. Tumor cells demonstrate finely granular nuclear chromatin and inconspicuous nuclei, distinguishing them from adenocarcinoma. (**d**) Photomicrograph of a typical carcinoid tumor with rosette formation
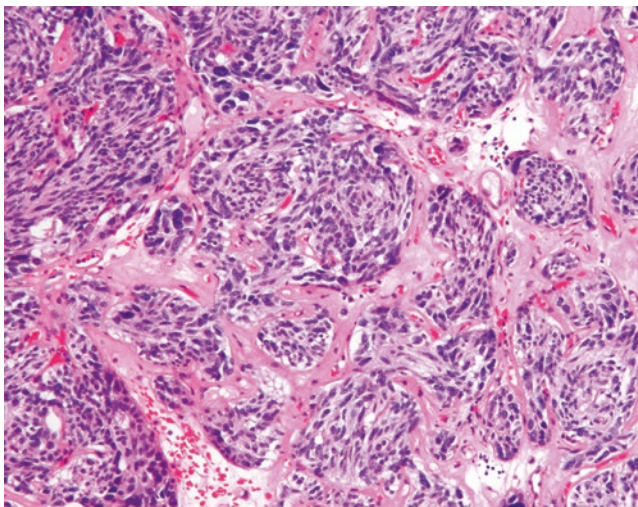
Fig. 13.26 Typical carcinoid tumor with prominent spindle cells. Photomicrograph showing a tumor composed of spindle cells with focally pronounced nuclear pleomorphism, which should not be taken as criteria for atypical carcinoid tumors. The tumor maintains a distinctly nested growth pattern without necrosis or mitotic figures
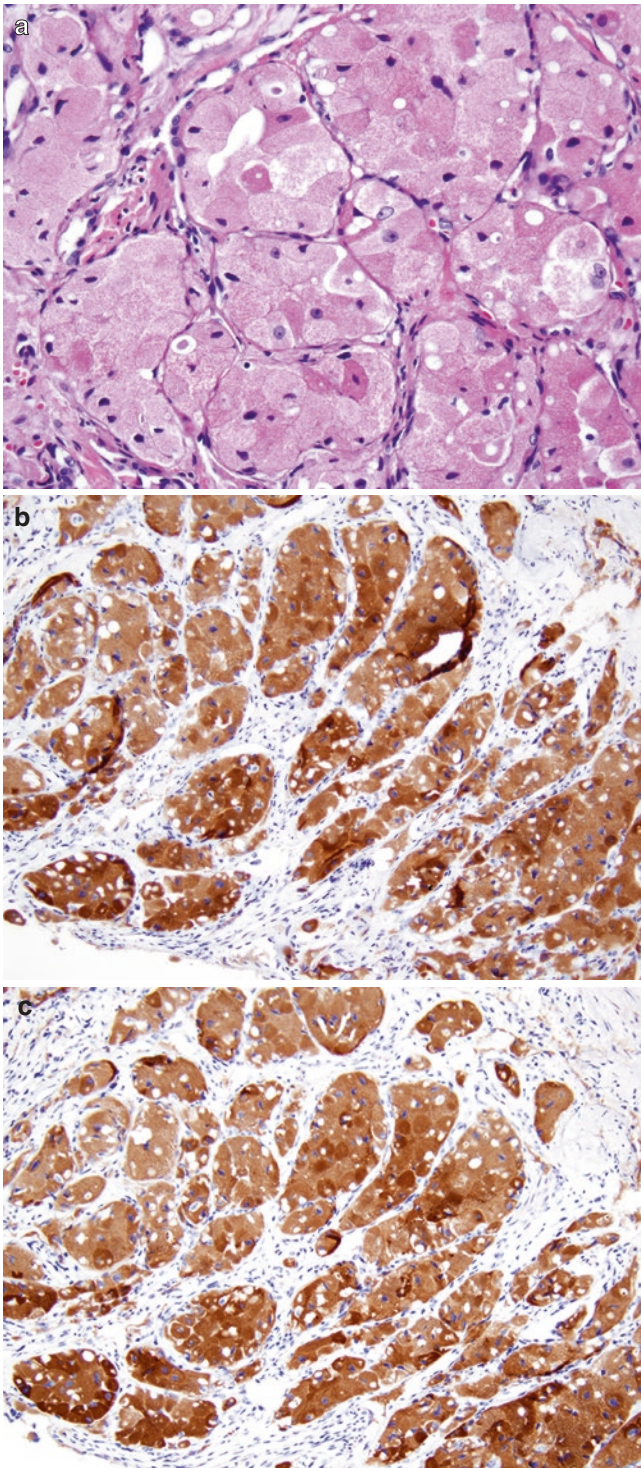
Fig. 13.27 Typical carcinoid tumor with oncocytic features. (**a**) Photomicrograph showing tumor cells with abundant eosinophilic granular cytoplasm and occasional prominent nucleoli on H&E stain. Immunohistochemical stains show strong cytoplasmic positivity for synaptophysin (**b**) and chromogranin (**c**)
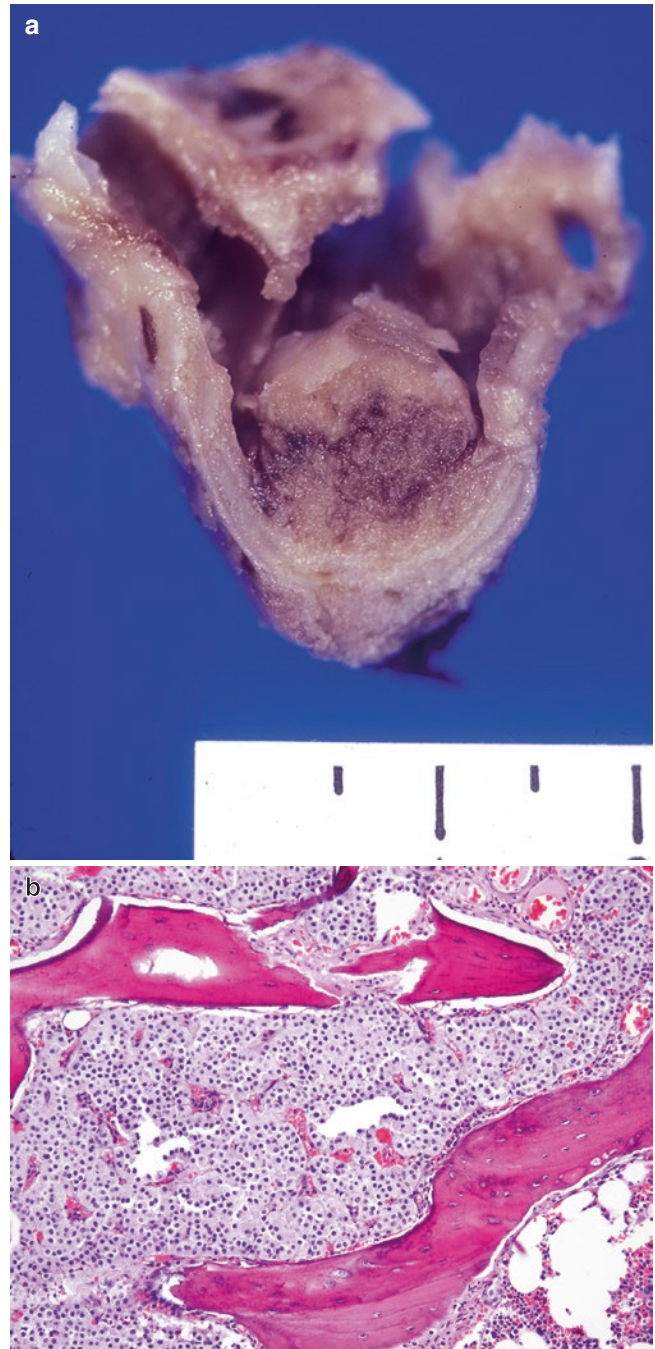
Fig. 13.28 Typical carcinoid tumor with ossification. (**a**) Gross photograph shows cut surface of heavily calcified endobronchial mass that required a saw to cut. (**b**) Photomicrograph shows osseous metaplasia of the stroma complete with bone marrow (lower right)

Fig. 13.31 Atypical carcinoid tumor. High-magnification photomicrograph shows a single mitotic figure in the center. Tumor cells show carcinoid morphology with a moderate amount of eosinophilic cytoplasm and finely granular nuclear chromatin

Table 13.3 Growth patterns seen in carcinoid tumors

Organoid nesting pattern
Trabecular pattern
Papillary pattern
Pseudoglandular or follicular pattern
Rosette formation

Fig. 13.29 Atypical carcinoid tumor. Gross photograph of a peripheral, well-circumscribed atypical carcinoid tumor measuring just over 3 cm in greatest dimension. There is no grossly detectable necrosis to distinguish this example from a low-grade typical carcinoid tumor. Microscopic necrosis and mitotic rate ($\geq$2/2 mm^2) are the features that separate atypical from typical carcinoid tumor

Table 13.4 Comparison between typical and atypical carcinoids

	Typical carcinoid	Atypical carcinoid
Histologic features	Neuroendocrine differentiation	
Mitosis	0–1 per 2 mm^2	2–10 per 2 mm^2
Necrosis	None	Focal, punctate necrosis
Prognosis	Excellent (90% 5-year survival)	Worse (60% 5-year survival)

Fig. 13.30 Atypical carcinoid tumor. Photomicrograph shows a carcinoid tumor with small foci of comedo-type necrosis in tumor nests

Small Cell Carcinoma

Small cell carcinoma (Figs. 13.32, 13.33, 13.34, 13.35, 13.36 and 13.37) is defined morphologically as a malignant epithelial neoplasm consisting of relatively small cells (about three times the diameter of a small lymphocyte) with scant cytoplasm, finely dispersed granular chromatin, absent or inconspicuous nucleoli, and nuclear molding. The high nuclear-cytoplasmic ratio (N:C) and nuclear characteristics are more helpful than cell size in distinguishing small cell carcinoma from other tumor types. The cells are often arranged in sheets without the "neuroendocrine architecture" characteristic of carcinoid tumors. Necrosis is universal, although small biopsies may not always reflect this finding. Mitotic figures are abundant ($>10/2$ mm^2). Neuroendocrine markers are commonly expressed but are not necessary for the diagnosis. The majority of small cell carcinomas are positive for TTF-1 and are generally negative or show only focal staining for p63 or p40 and high molecular weight cytokeratins (i.e., CK5/6). This immunophenotype can be helpful in distinguishing small cell carcinoma from basaloid variants of squamous cell carcinoma, especially in small biopsies. Ki67 labeling indices are usually very high, which is useful in separating small cell carcinoma from typical and atypical carcinoid tumors in small biopsies, especially those with crush artifact.

Fig. 13.32 Small cell carcinoma. Gross photograph of autopsy specimen showing small cell carcinoma distributed as a large centrally located mass involving the major bronchi, with bulky lymph node metastases
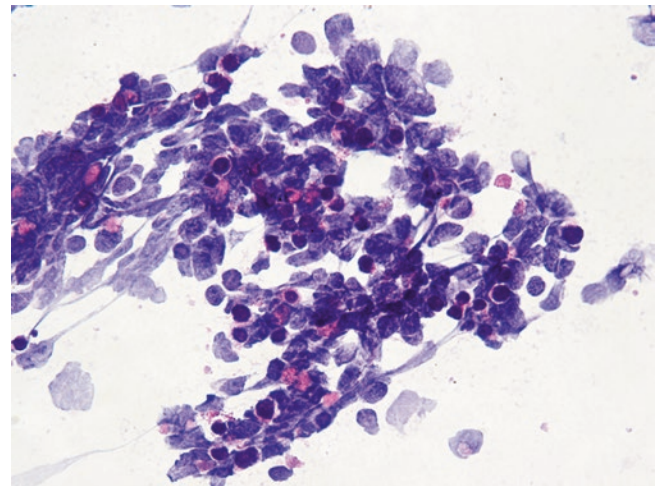
Fig. 13.33 Small cell carcinoma. High-magnification photomicrograph illustrating the distinctive cytologic features of small cell carcinoma in a smear prepared from a fine needle aspirate. Tumor cells show very scant cytoplasm, hyperchromatic nuclei, finely dispersed "salt and pepper" chromatin, absent nucleoli, nuclear molding, and prominent apoptosis. Cytology specimens can be extremely helpful in patients whose bronchial biopsies show extensive crush artifact
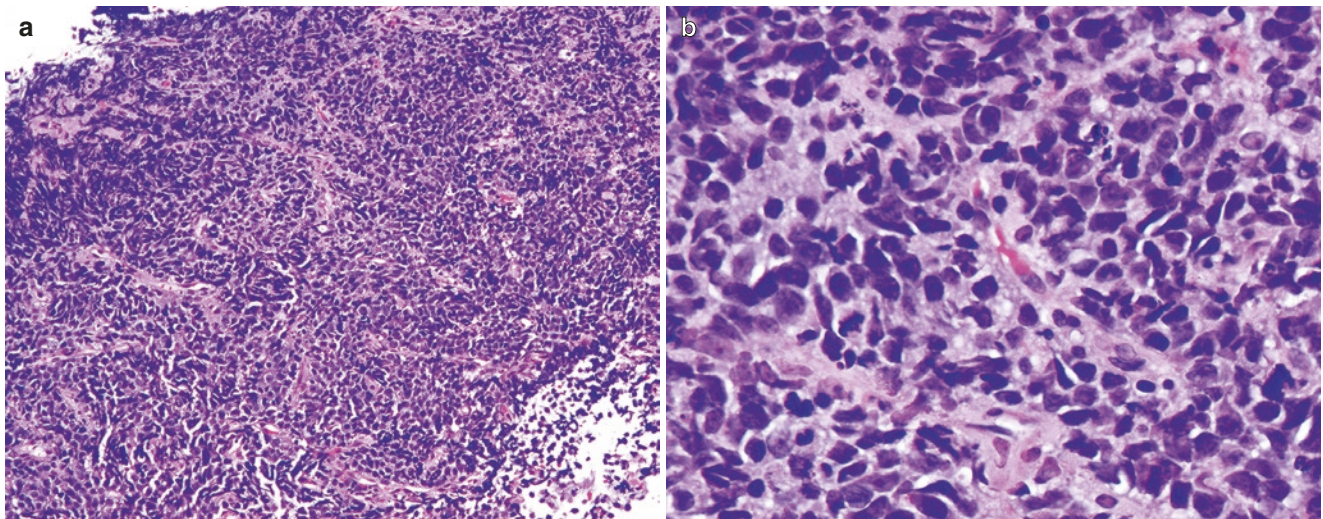
Fig. 13.34 Small cell carcinoma. (**a**) Low-magnification photomicrograph shows densely packed small- to intermediate-sized tumor cells. Crushing artifact is seen at the upper-left edge. (**b**) High-magnification view showing tumor cells with scant cytoplasm, dense chromatin, and occasional small nucleoli. Mitoses and apoptosis are frequently seen
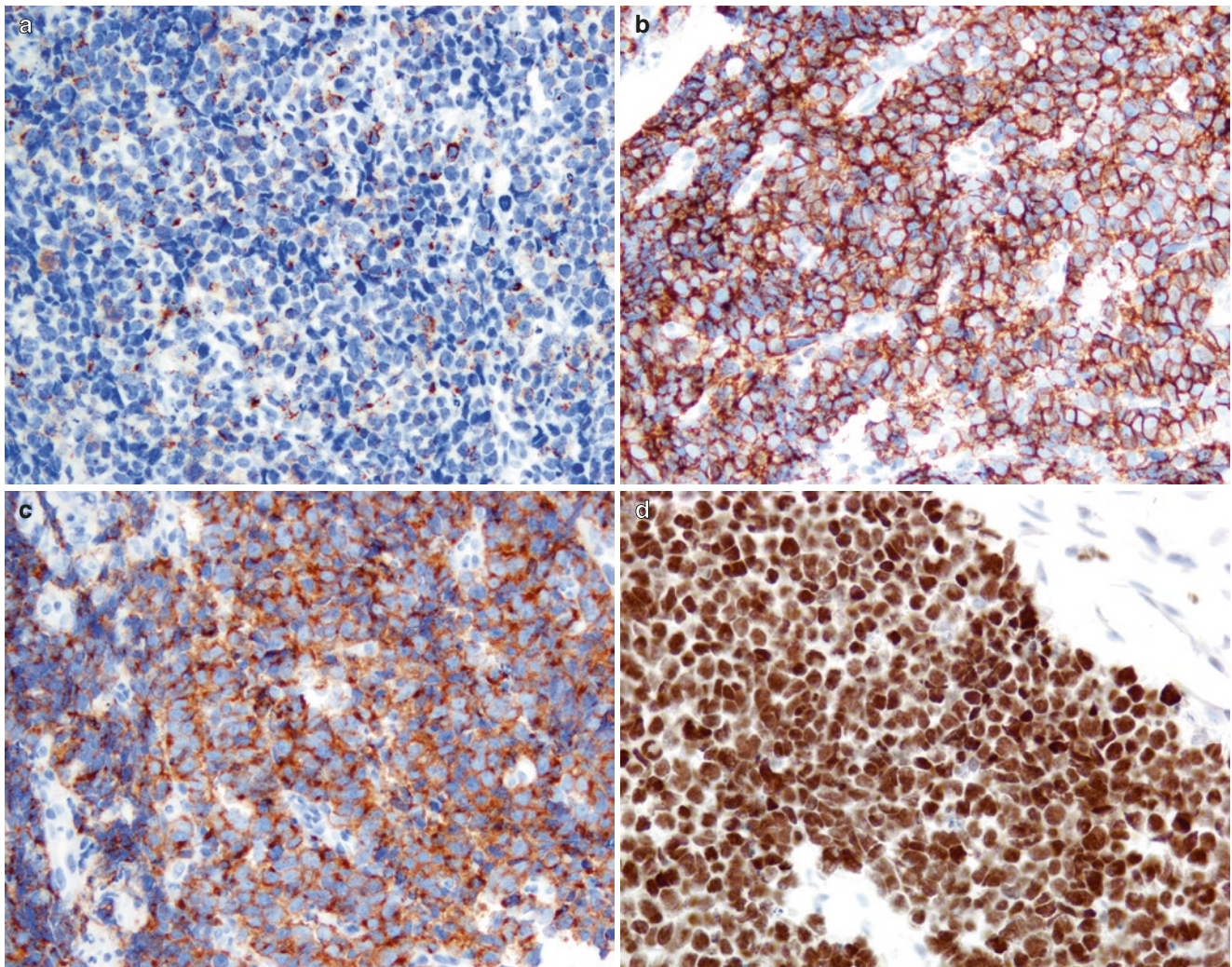
Fig. 13.35 Small cell carcinoma. (**a–d**), Photomicrographs of immunostained slides showing characteristic cytoplasmic perinuclear dot-like staining for cytokeratin (AE1/AE3) (**a**), diffuse membranous and cytoplasmic staining for CD56 (**b**), cytoplasmic staining for synaptophysin (**c**), and nuclear staining for TTF-1 (**d**). Not all small cell carcinomas show all of these features, including rare examples with a "null" phenotype. Absence of staining for CD20 and p63/p40 can be extremely helpful, especially in those with an otherwise "null" phenotype, in separating small cell carcinoma from lymphomas and basaloid squamous cell carcinomas on small biopsies
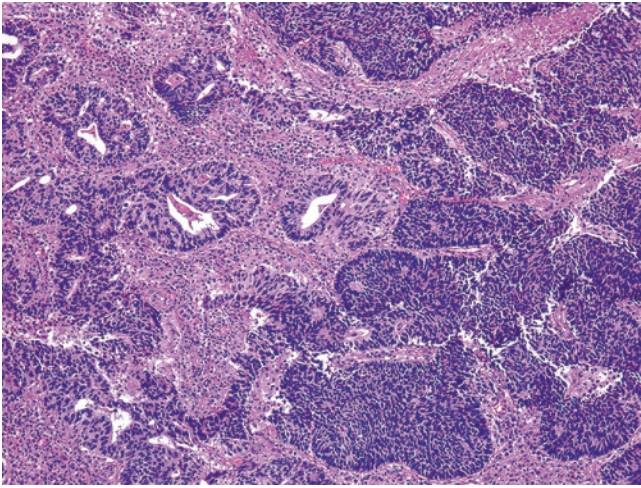
Fig. 13.36 Combined small cell carcinoma and adenocarcinoma. Photomicrograph showing malignant glands with cribriform architecture (*left*) immediately next to small cell carcinoma (*right*)
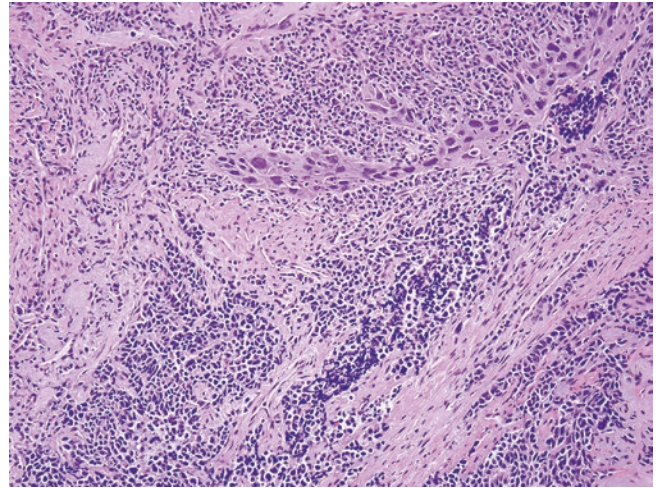
Fig. 13.37 Combined small cell carcinoma and squamous cell carcinoma. Photomicrograph showing a nest of squamous cell carcinoma consisting of polygonal cells with prominent intercellular bridging and occasional single dyskeratotic cells situated in the midst of an otherwise classic small cell carcinoma

Large Cell Neuroendocrine Carcinoma

Large cell neuroendocrine carcinoma (Figs. 13.38, 13.39 and 13.40) is defined as a high-grade malignant epithelial tumor with neuroendocrine growth patterns (i.e., the growth patterns characteristically seen in carcinoid tumors), cytologic features more closely resembling those seen in non-small cell carcinomas (i.e., large nucleoli and more abundant cytoplasm without nuclear molding), and immunohistochemical staining for neuroendocrine mark- ers. Necrosis is universal and tends to be more extensive than the necrosis seen in atypical carcinoid tumors. Lung carcinomas with carcinoid morphology but more than ten mitoses per 2 mm^2 are better classified as large cell neuroendocrine carcinomas according to the 2015 WHO classification. There is significant histologic overlap with small cell carcinoma, which accounts for the relatively low rates of interobserver agreement even among experts in distinguishing these highly related variants of high-grade neuroendocrine carcinoma.
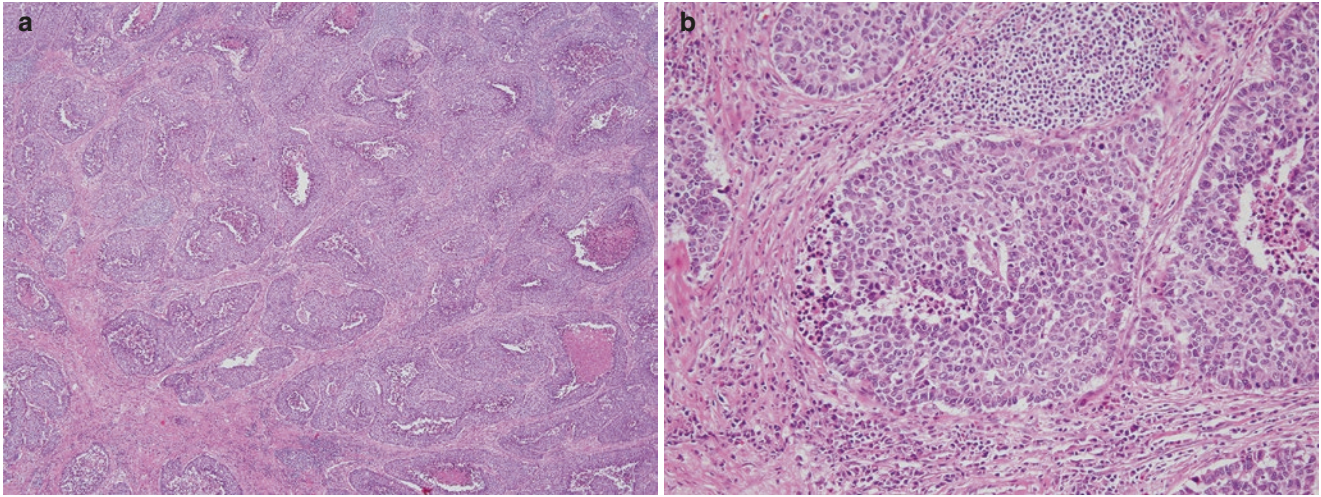
Fig. 13.38 Large cell neuroendocrine carcinoma. (**a**) Low-magnification photomicrograph shows a nested growth pattern with peripheral palisading and multifocal "comedo" necrosis situated centrally within the cell nests. The necrotic foci are much more extensive than that usually seen in atypical carcinoid tumors. (**b**) Higher-magnification view showing a tumor nest with peripheral palisading and foci of necrosis. The tumor cells show vesicular chromatin and abundant eosinophilic cytoplasm. Numerous mitoses are seen
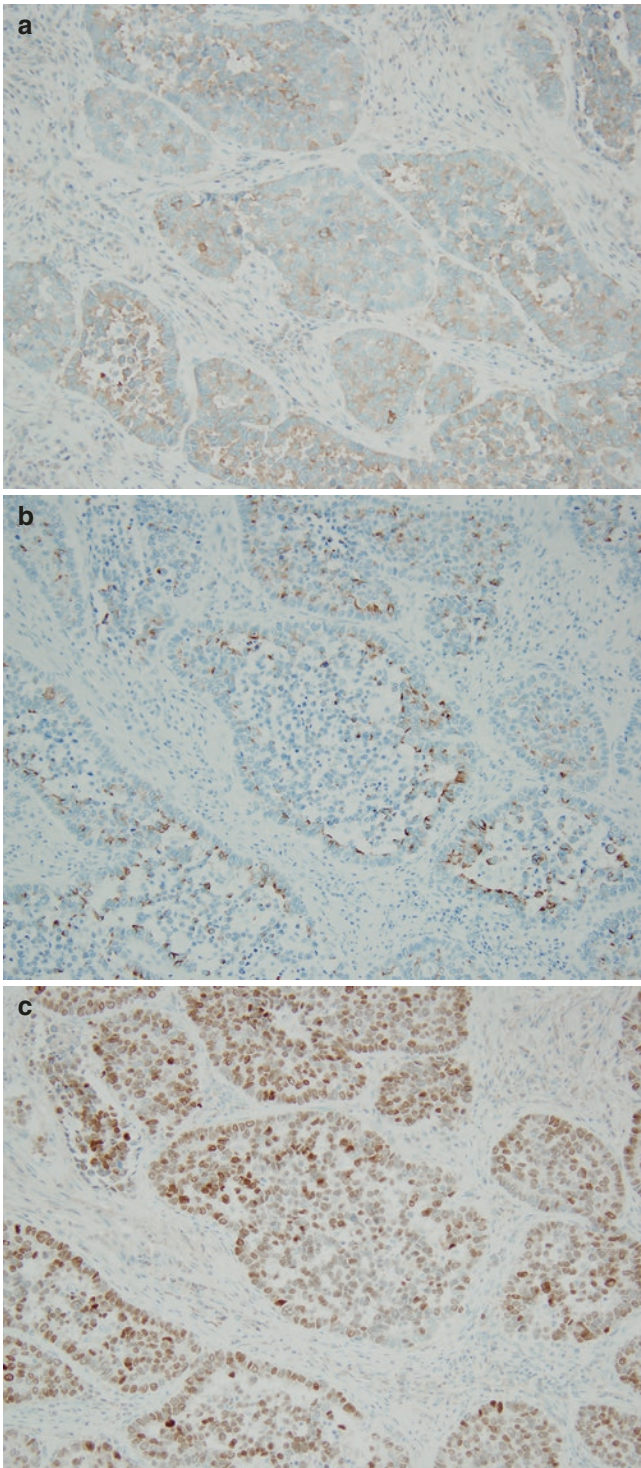
Fig. 13.39 Immunostaining of large cell neuroendocrine carcinoma. (**a**–**c**), A series of photomicrographs of immunostained sections from the tumor illustrated in Fig. 13.38 showing patchy cytoplasmic staining for synaptophysin (**a**) and chromogranin (**b**) and nuclear staining for TTF-1 in isolated tumor cells (**c**). TTF-1 immunoreactivity is not a consistent feature of large cell neuroendocrine carcinoma
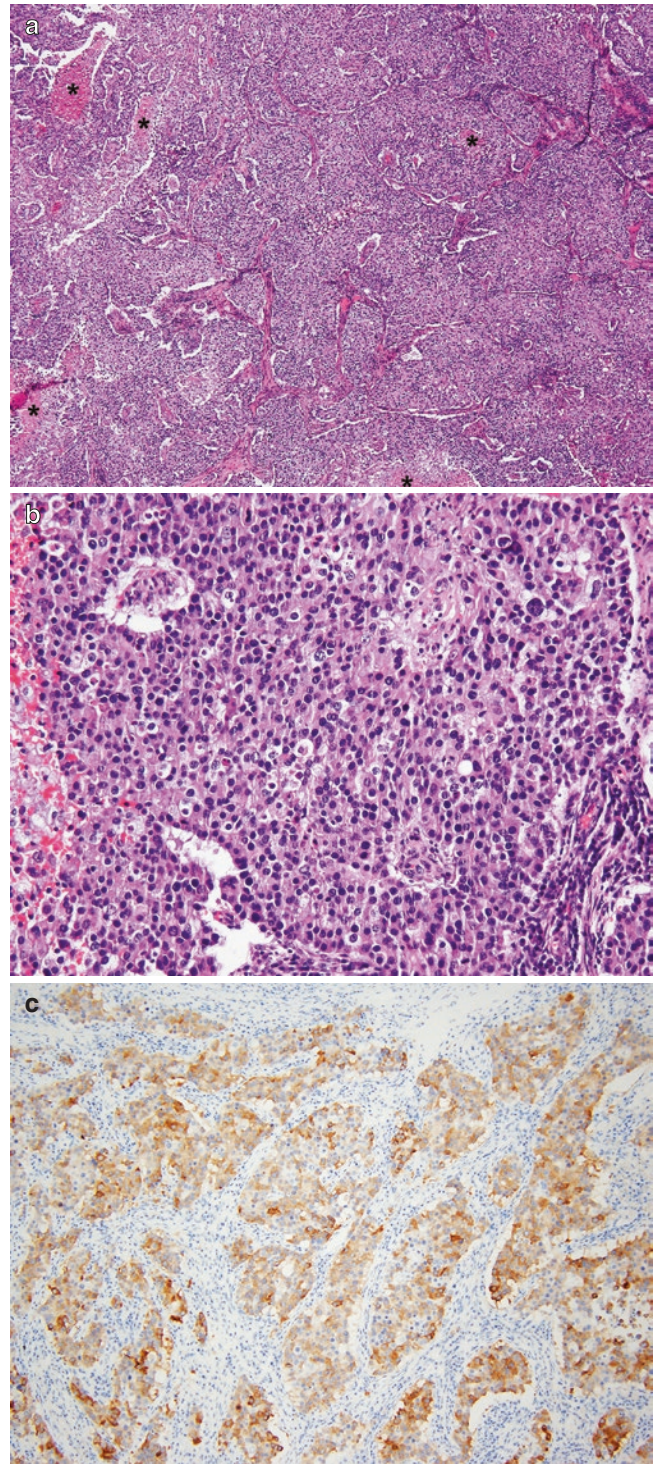
Fig. 13.40 Large cell neuroendocrine carcinoma. (**a**) Low-magnification photomicrograph showing another example of large cell neuroendocrine carcinoma with a nested growth pattern mimicking carcinoid tumor but with multifocal coagulative tumor necrosis (asterisk). (**b**) Higher-magnification photomicrograph showing coarse chromatin and easily identifiable nucleoli in tumor cells with abundant eosinophilic cytoplasm. Numerous mitotic figures are present. (**c**) Photomicrograph of an immunostained section shows diffuse immunoreactivity for synaptophysin. Tumor cells were also positive for CD56 but were negative for chromogranin (not shown)

Large Cell Carcinoma

Large cell carcinoma (Figs. 13.41 and 13.42) is undifferentiated non-small cell carcinoma lacking morphologic and immunohistochemical features of any other specific types and is therefore always a diagnosis of exclusion. For that reason, the diagnosis is made only after thorough examination of a resected tumor. Defined in this way, large cell carcinoma typically is composed of large polygonal cells with coarse or vesicular chromatin, prominent nucleoli, and abundant cytoplasm. The cells are arranged in sheets without distinct architectural features. Often the differential diagnosis on the basis of histology alone includes large cell or anaplastic lymphomas and melanoma. Immunostains are helpful in establishing an epithelial origin and are by definition negative for markers affiliated with adenocarcinoma (TTF-1, napsin A) and squamous cell carcinoma (CK5/6, p63, p40).
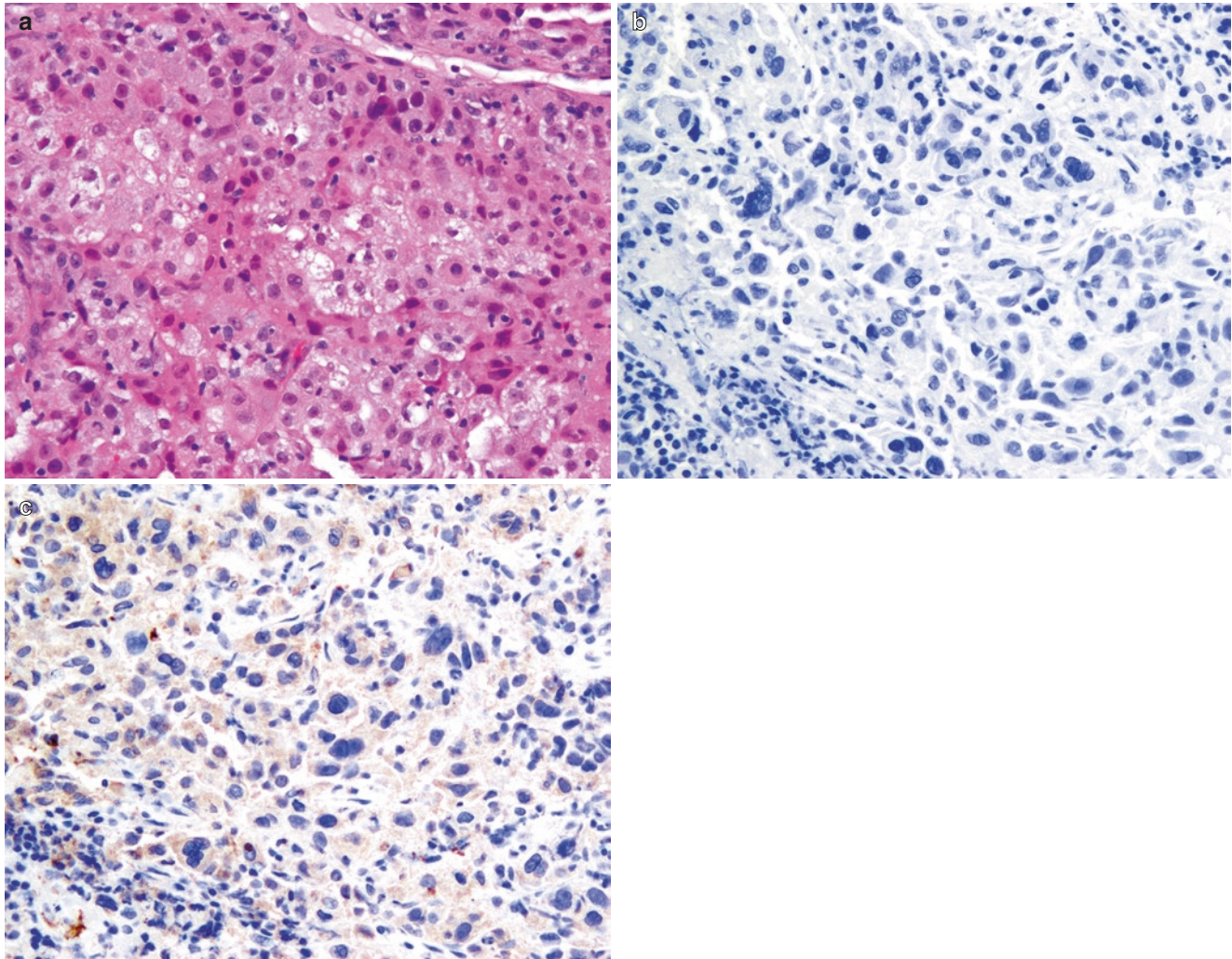
Fig. 13.41 Large cell carcinoma. (**a**) Photomicrograph showing sheets of large polygonal cells with prominent nucleoli and abundant finely vacuolated clear to eosinophilic cytoplasm on H&E stain. By definition, the tumor lacks staining for markers of squamous differentiation such as p40 (**b**) and markers affiliated with adenocarcinoma such as TTF-1 (**c**)
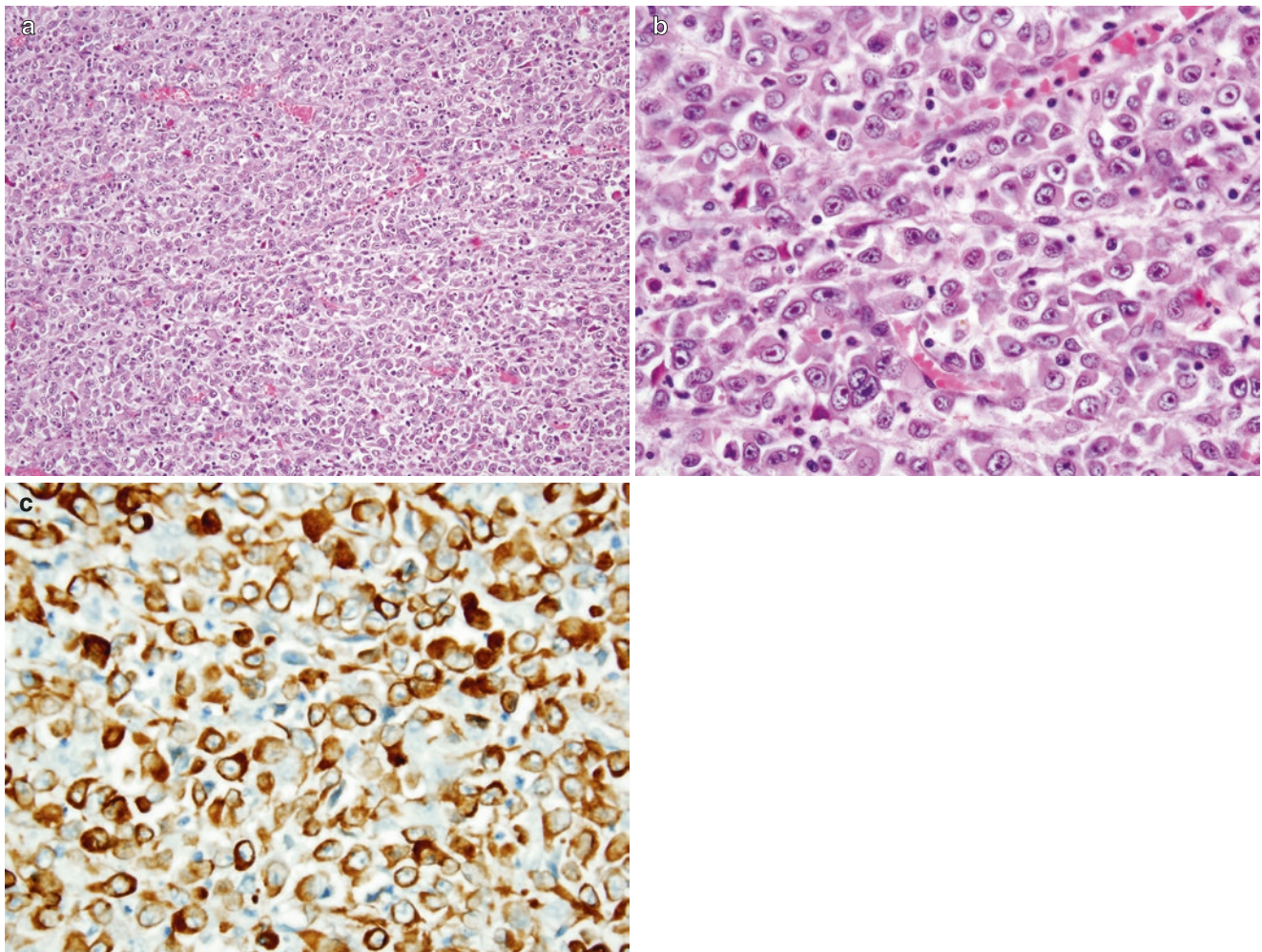
Fig. 13.42 Large cell carcinoma. (**a**) Photomicrograph showing high-grade carcinoma in which large polygonal cells are discohesive and arranged in sheets without evidence of glandular or squamous differentiation. (**b**) High-magnification view shows vesicular chromatin with giant solitary nucleoli and an eccentric rim of densely eosinophilic cytoplasm. Based on these findings alone, the differential diagnosis is likely to include not only large cell carcinoma but also other pleomorphic high-grade tumors such as anaplastic large cell lymphoma and melanoma. (**c**) High-magnification photomicrograph showing strong cytoplasmic staining using a pancytokeratin cocktail (AE1/AE3 and CAM5.2). Tumor cells were negative for all other markers tested including TTF-1, napsin A, CK5/CK6, and p63 (not shown)

Sarcomatoid Carcinoma

Sarcomatoid carcinoma (Figs. 13.43, 13.44, 13.45, 13.46, 13.47, 13.48, 13.49, 13.50 and 13.51) is a general term applied to high-grade variants of non-small cell carcinoma in which at least a portion of the tumor has histologic features resembling nonepithelial sarcomas.

Sarcomatoid carcinomas may or may not have a clearly identifiable epithelial component with histologic features indistinguishable from conventional carcinoma subtypes such as adenocarcinoma, squamous cell carcinoma, and/or large cell carcinoma. Rare examples of sarcomatoid carcinoma have a component of small cell carcinoma (e.g., "combined small cell and spindle-cell carcinoma"). Tumors that comprise both sarcomatoid and conventional carcinomatous components are often referred to as biphasic and are termed carcinosarcoma if the sarcomatous component duplicates the features of a classifiable sarcoma type such as osteosarcoma, chondrosarcoma, or rhabdomyosarcoma. Other variants of sarcomatoid carcinoma included under this generic heading may be specified as spindle-cell carcinomas, giant cell carcinomas, pleomorphic carcinomas (which are distinguished by a combination of spindle cells and giant cells with or without a conventional carcinomatous component), and pulmonary blastomas.

Subclassifying high-grade sarcomatoid carcinoma into these subtypes has little if any clinical significance but can be helpful in thinking about the differential diagnosis. Most nonscreening-detected sarcomatoid carcinomas present as large, centrally necrotic masses (high T stage) with paradoxically low rates of nodal or distant metastases (low N and M stage) at the time of diagnosis. The natural history tends to be an aggressive course with low survival rates.

Fig. 13.43 Sarcomatoid carcinoma. Photograph illustrating cut surface of a large centrally necrotic sarcomatoid carcinoma. (Courtesy of Dr. J. Carvalho, Minneapolis, MN)
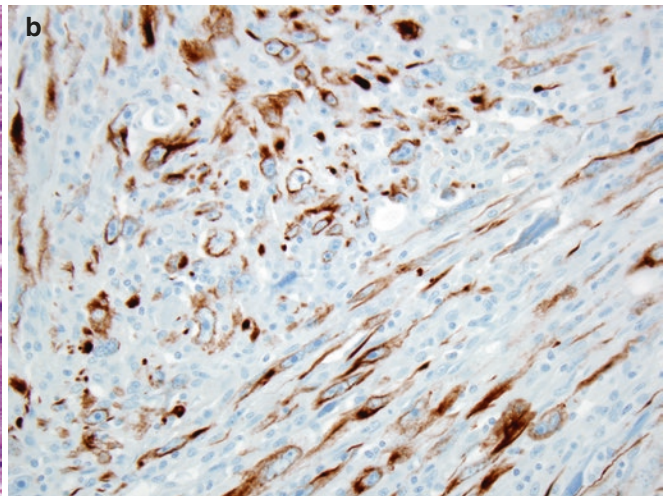
Fig. 13.44 Pleomorphic carcinoma. (**a**) High-magnification photomicrograph demonstrates an undifferentiated carcinoma with large bizarre nuclei, multinucleated giant cells, and spindle cells. (**b**) High-magnification photomicrograph showing that tumor cells are positive for pancytokeratins (AE1/AE3) but were negative for TTF-1 and p63 (not shown)
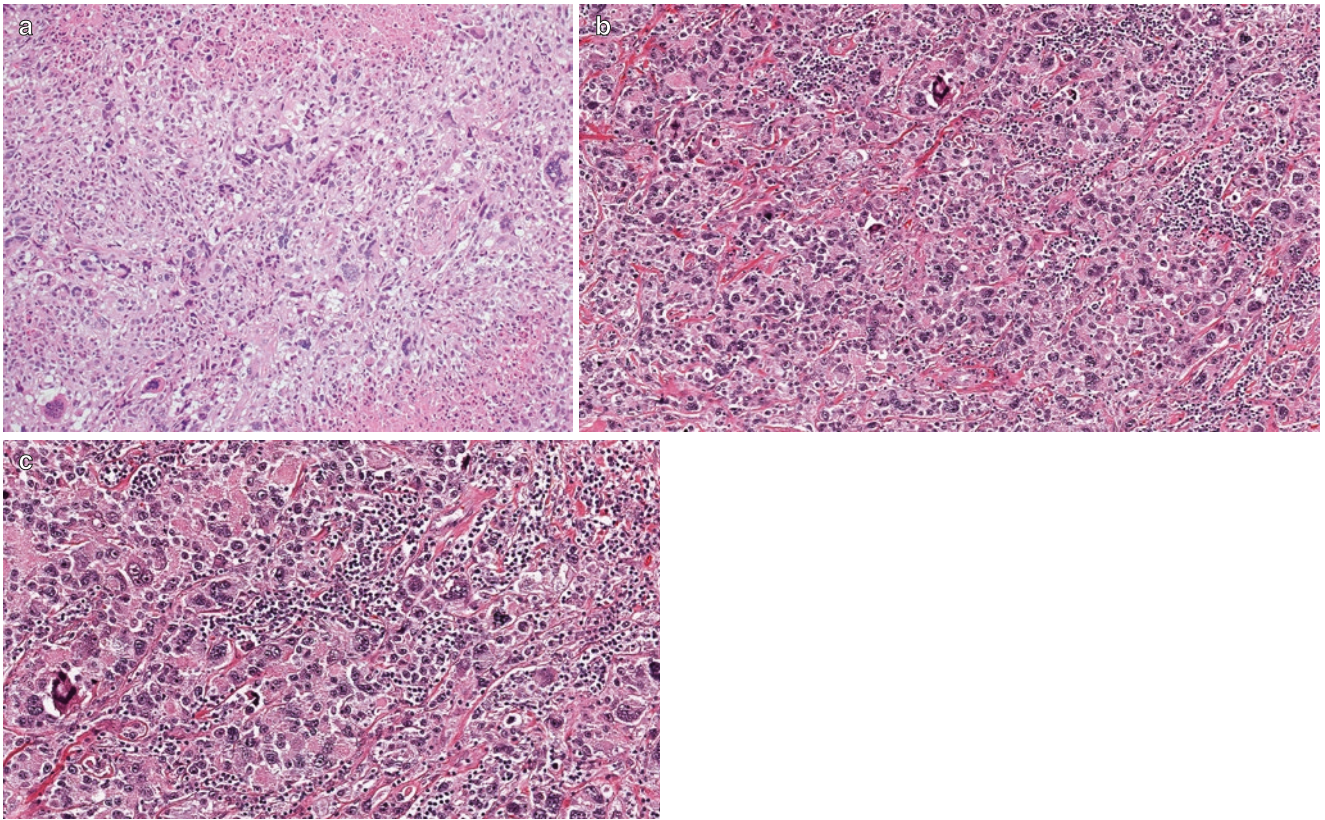
Fig. 13.45 Pleomorphic and giant cell carcinoma. (**a**) Photomicrograph showing a high-grade non-small cell carcinoma with prominent multi-nucleated giant cells. (**b**) and (**c**), Photomicrographs of a "pure" giant cell carcinoma, an extremely rare variant of sarcomatoid carcinoma that is associated with an extremely aggressive course
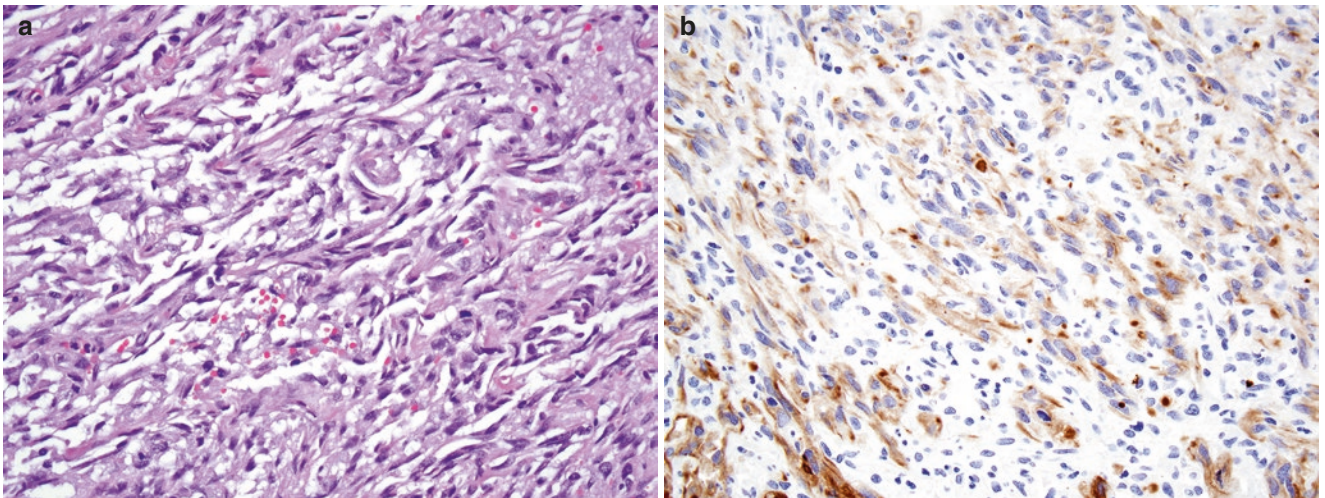
Fig. 13.46 Spindle-cell carcinoma. (**a**) High-magnification photomicrograph showing a tumor consisting entirely of spindle cells. The tumor cells are relatively uniform, growing in fascicles and whorls with surprisingly mild cytologic atypia. (**b**) High-magnification view of immunostained section showing that the spindle cells are positive for pancytokeratins (AE1/AE3)
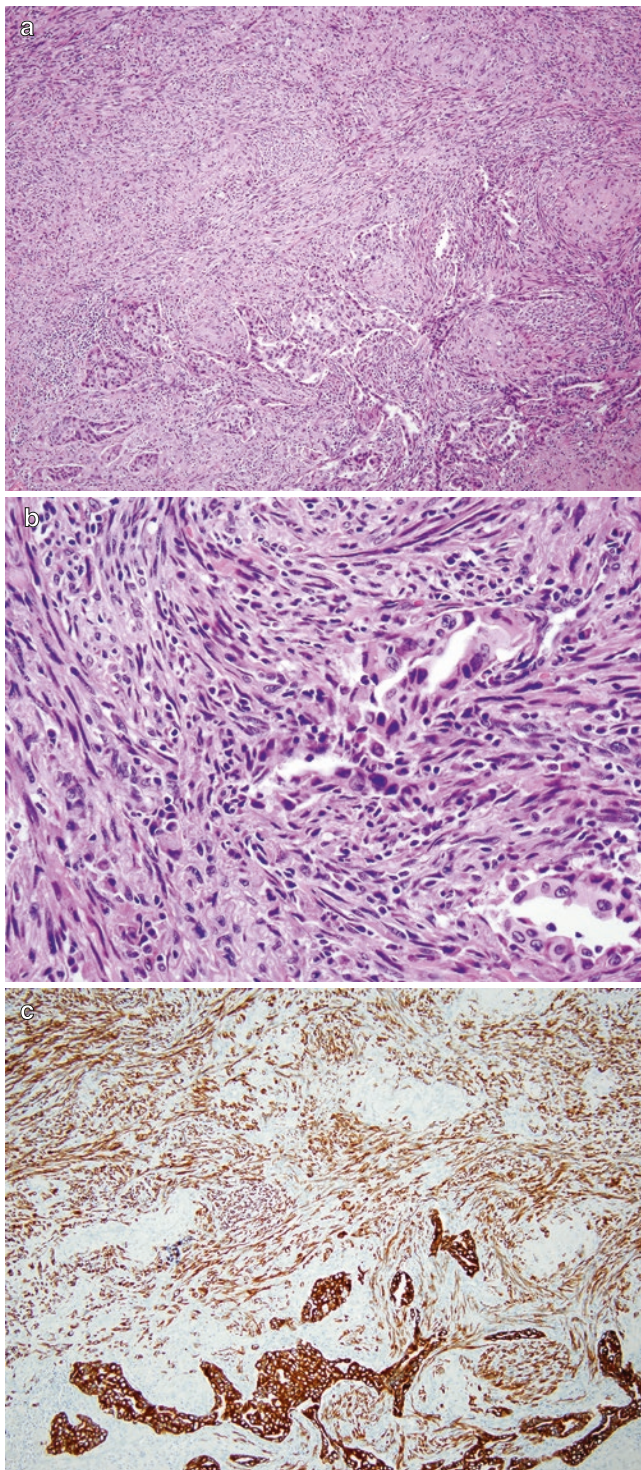
Fig. 13.47 Spindle-cell carcinoma with adenocarcinoma. (**a**) Low-magnification photomicrograph showing a tumor consisting of both spindle cells (at least 10% of the tumor) and adenocarcinoma with an acinar and cribriform growth pattern. (**b**) Higher-magnification photomicrograph showing an intimate admixture of neoplastic glands and spindle cells. (**c**) Photomicrograph of immunostained sections showing that both spindle-cell and glandular components are positive for pancytokeratins (AE1/AE3)
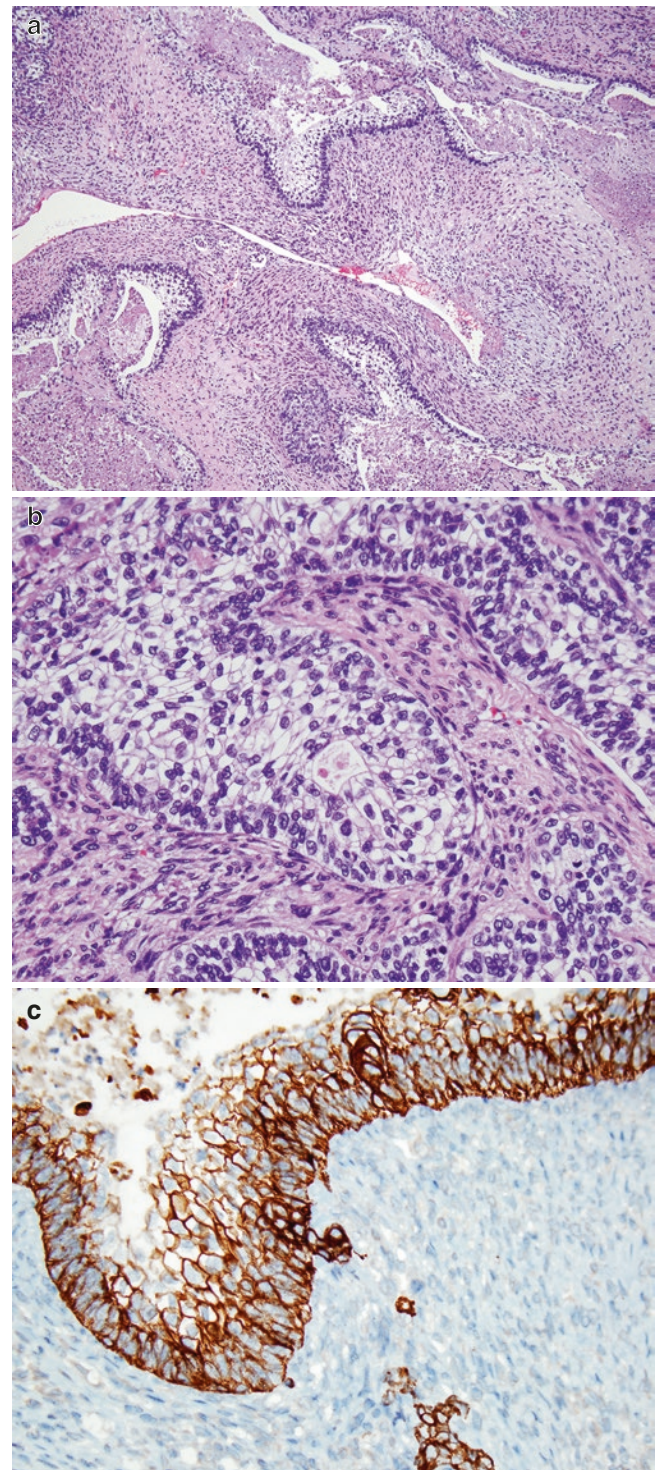
Fig. 13.48 Spindle-cell carcinoma with squamous cell carcinoma. (**a**) Low-magnification view of large, necrotizing, polypoid endobronchial tumor consisting of a combination of spindle cells (at least 10% of the tumor) and squamous cell carcinoma with clear cell change. (**b**) High-magnification photomicrograph showing squamous cell carcinoma in which polygonal cells have abundant clear cytoplasm and are arranged in a well-developed epidermoid growth pattern without keratinization. (**c**) High-magnification view of immunostained section shows staining for high molecular weight cytokeratins (CK5/6) limited to the squamous component. A stain for p63 showed the same distribution (not shown)
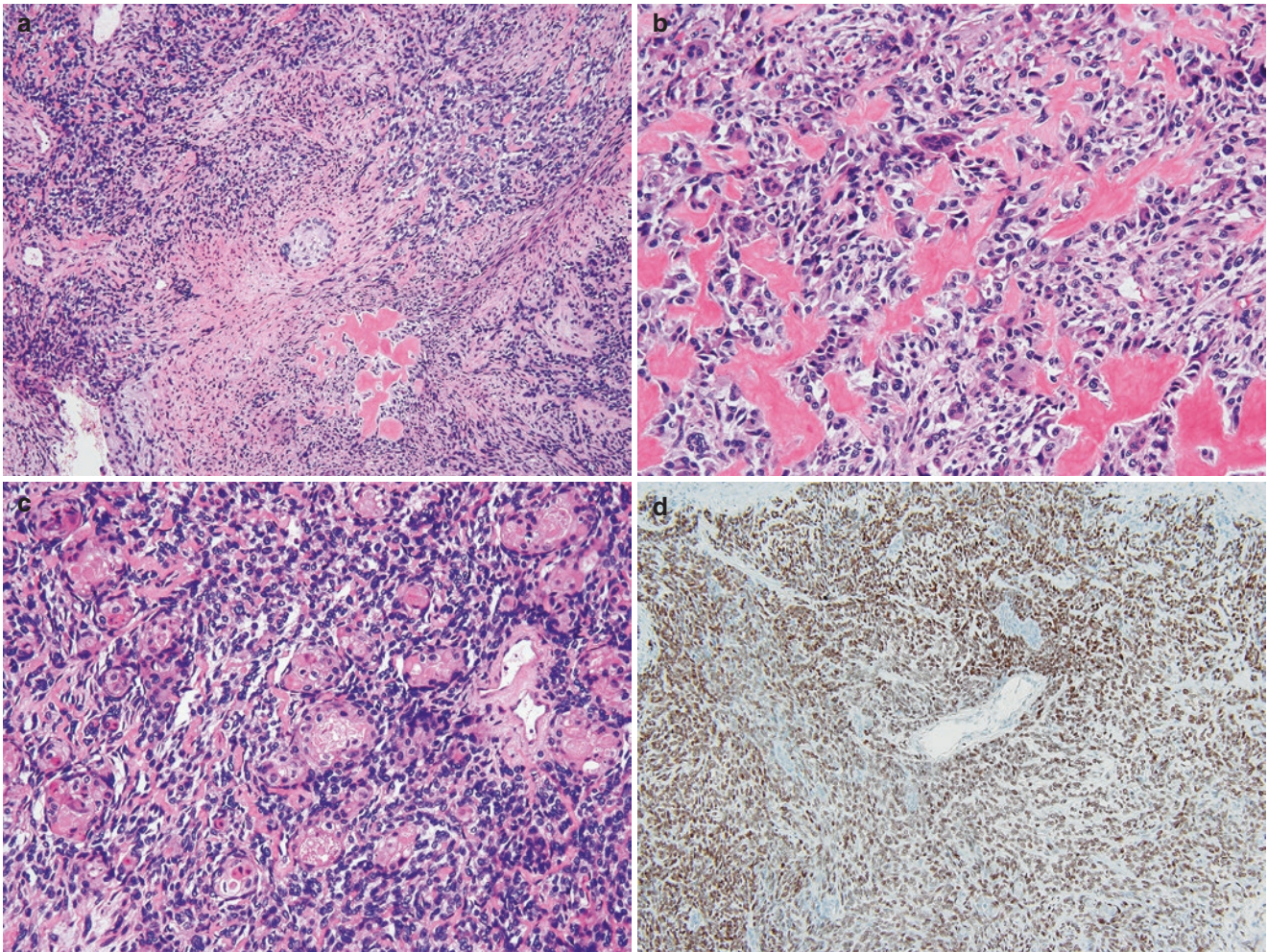
Fig. 13.49 Carcinosarcoma. (**a**) Photomicrograph of a tumor with admixed squamous cell carcinoma and both sarcomatoid (spindle-cell) and sarcomatous (osteosarcoma) components. (**b**) High-magnification view of differentiated sarcomatous component closely resembling osteosarcoma with spicules of neoplastic osteoid affiliated with undifferentiated neoplastic and osteoclast-like giant cells. (**c**) High-magnification view of the carcinomatous component in which there is abrupt squamous differentiation in the form of keratinizing squamous pearls. (**d**) Photomicrograph of immunostained sections showing that much of the tumor, including relatively undifferentiated spindle cells, was positive for p63
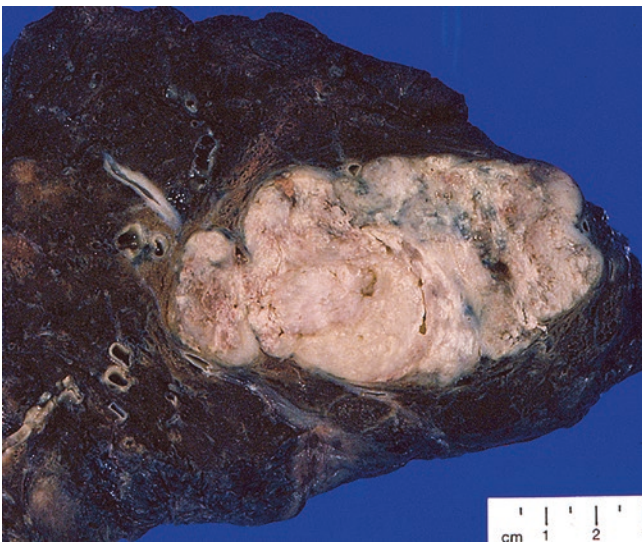
Fig. 13.50 Pulmonary blastoma. Gross photograph showing cut surface of a large, well-circumscribed pulmonary blastoma with patchy necrosis
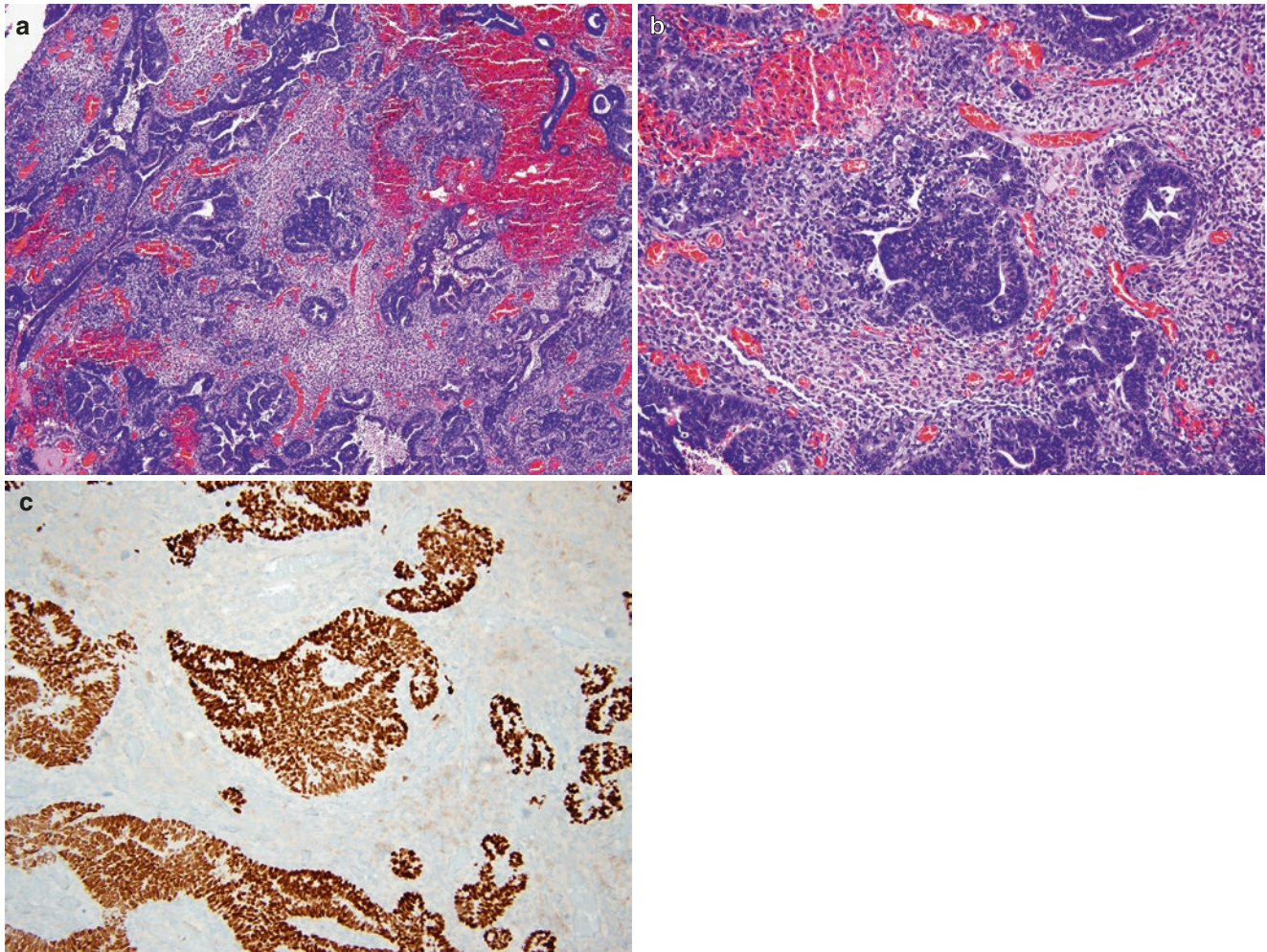
Fig. 13.51 Pulmonary blastoma. (**a**) Photomicrograph showing a biphasic tumor consisting of an adenocarcinoma resembling endometrioid carcinoma and a primitive ("blastematous") stromal component. (**b**) Higher-magnification photomicrograph showing pseudostratified non-mucinous columnar cells with a well-developed acinar and cribriform growth pattern. Associated morules may also be present, furthering the resemblance to endometrioid carcinomas. When present in pure form without the primitive stromal component, the "monophasic" epithelial component is termed fetal adenocarcinoma. (**c**) Photomicrograph of an immunostained section showing strong staining of the adenocarcinomatous component for TTF-1 with negative staining in the stromal component. The stromal cells are usually negative for TTF-1 and are also frequently negative for cytokeratins

Salivary Gland-Type Carcinomas

Salivary gland-type carcinomas (Figs. 13.52, 13.53, 13.54, 13.55, 13.56, 13.57 and 13.58) are generally rare and usually present as central tumors arising from cartilaginous airways.

Common types include mucoepidermoid carcinoma and adenoid cystic carcinoma. Other rare variants, including primary mammary analogue secretory carcinoma, have also been reported.
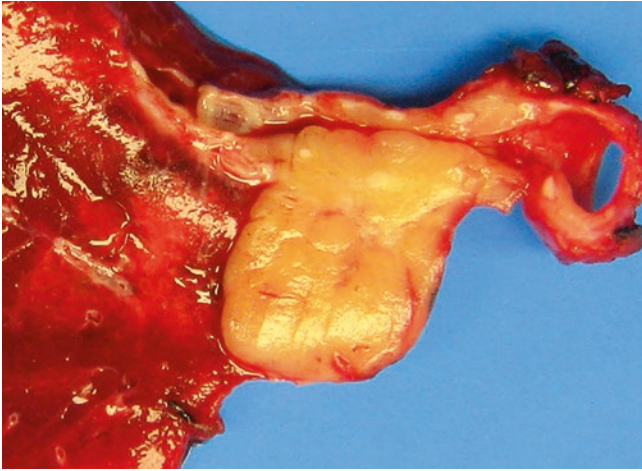
Fig. 13.52 Adenoid cystic carcinoma. Gross photograph of sleeve resection for adenoid cystic carcinoma. The tumor extensively infiltrates the submucosal tissues, extending beyond the airway cartilage to form a well-defined unencapsulated peribronchial mass
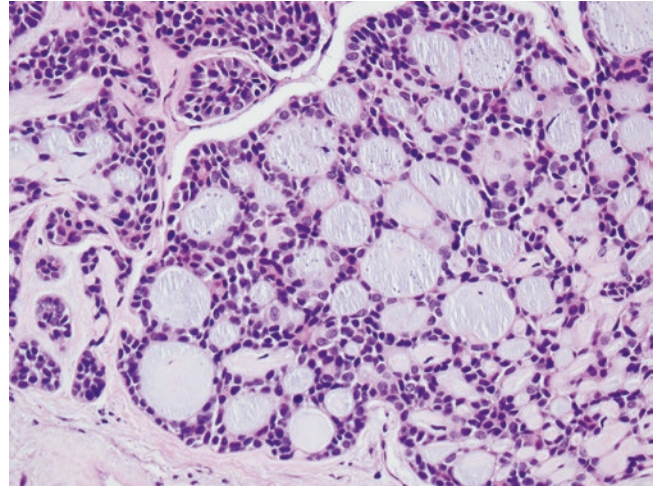
Fig. 13.54 Adenoid cystic carcinoma. High-magnification photomicrograph of another example showing classic cribriform architecture in which small tumor cells with scant cytoplasm and angulated hyperchromatic nuclei constitute the majority of the neoplasm with only scattered ductal epithelial cells with eosinophilic cytoplasm. No mitosis or necrosis is seen. The cribriform structure is created by pale-staining extracellular myxoid secretions accumulated within pseudoglandular spaces ("pseudocysts"). The stroma is fibrotic, with focal areas of eosinophilic basement membrane-like materials (upper left)

Fig. 13.53 Adenoid cystic carcinoma. (**a**) Low-magnification photomicrograph shows a tumor with a predominantly tubular growth pattern diffusely involving the bronchial wall and infiltrating into peribronchial soft tissue. (**b**) A higher-magnification view shows characteristic small myoepithelial cells with hyperchromatic angulated nuclei and occasional central clusters of cytologically distinct ductal epithelial cells. This tumor shows the characteristic pattern of associated extracellular pseudoglandular spaces containing granular and pale-staining basophilic myxoid secretions

Fig. 13.55 Adenoid cystic carcinoma. Photomicrograph of an immunostained section shows that tumor cells may be focally positive for TTF-1

Fig. 13.56 Mucoepidermoid carcinoma. Gross photograph showing the cut surface of a well-demarcated polypoid endobronchial mass. Note that the tumor is focally cystic and affiliated with "golden [obstructive] pneumonia" at lower left. (Courtesy of J. Carvalho, Minneapolis, MN)
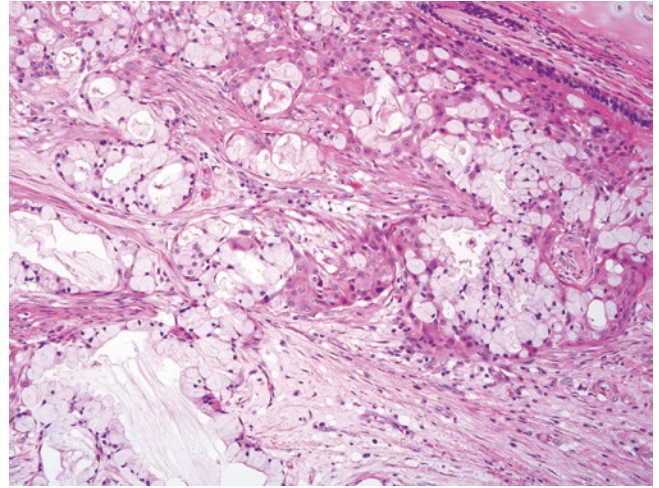
Fig. 13.58 Mucoepidermoid carcinoma. Photomicrograph of another mucoepidermoid carcinoma showing dramatic admixture of mucinous goblet cells and squamoid "intermediate" cells
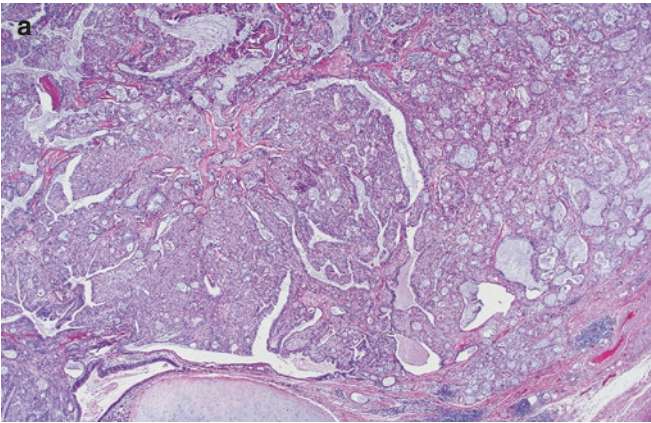
Fig. 13.57 Mucoepidermoid carcinoma. (**a**) Low-magnification photomicrograph shows an endobronchial tumor with mixed solid and cystic growth patterns. The cystic areas are affiliated with variably abundant extracellular mucin. (**b**) High-magnification view shows solid nests composed of a mixture of cuboidal "intermediate" cells and mucinous goblet cells
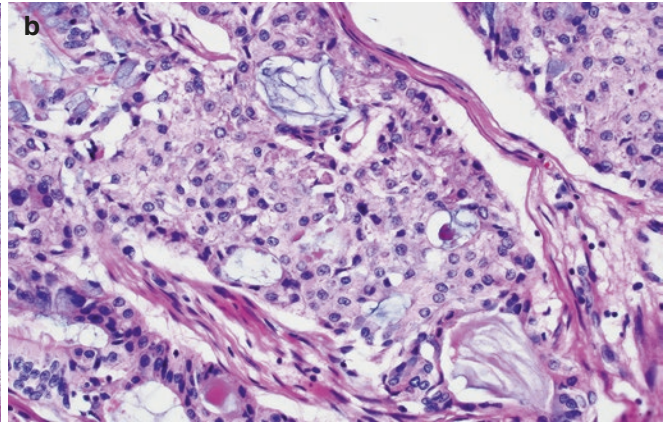
Suggested Reading

Brambilla E, Moro D, Veale D, Brichon PY, Stoebner P, Paramelle B, et al. Basal cell (basaloid) carcinoma of the lung: a new morphologic and phenotypic entity with separate prognostic significance. Hum Pathol. 1992;23:993–1003.

Kadota K, Villena-Vargas J, Yoshizawa A, Motoi N, Sima CS, Riely GJ, et al. Prognostic significance of adenocarcinoma in situ, minimally invasive adenocarcinoma, and nonmucinous lepidic predominant invasive adenocarcinoma of the lung in patients with stage I disease. Am J Surg Pathol. 2014;38:448–60.

Kitamura H, Kameda Y, Ito T, Hayashi H. Atypical adenomatous hyperplasia of the lung. Implications for the pathogenesis of peripheral lung adenocarcinoma. Am J Clin Pathol. 1999;111:610–22.

Koss MN, Hochholzer L, O'Leary T. Pulmonary blastomas. Cancer. 1991;67:2368–81.

Maziak DE, Todd TR, Keshavjee SH, Winton TL, Van Nostrand P, Pearson FG. Adenoid cystic carcinoma of the airway: thirty-two-year experience. J Thorac Cardiovasc Surg. 1996;112:1522–31. discussion 1531–22

Mori M, Rao SK, Popper HH, Cagle PT, Fraire AE. Atypical adenomatous hyperplasia of the lung: a probable forerunner in the development of adenocarcinoma of the lung. Mod Pathol. 2001;14:72–84.

Nakatani Y, Kitamura H, Inayama Y, Kamijo S, Nagashima Y, Shimoyama K, et al. Pulmonary adenocarcinomas of the fetal lung type: a clinicopathologic study indicating differences in histology, epidemiology, and natural history of low-grade and high-grade forms. Am J Surg Pathol. 1998;22:399–411.

Nicholson SA, Beasley MB, Brambilla E, Hasleton PS, Colby TV, Sheppard MN, et al. Small cell lung carcinoma (SCLC): a clinicopathologic study of 100 cases with surgical specimens. Am J Surg Pathol. 2002;26:1184–97.

Roden AC, Garcia JJ, Wehrs RN, Colby TV, Khoor A, Leslie KO, et al. Histopathologic, immunophenotypic and cytogenetic features of pulmonary mucoepidermoid carcinoma. Mod Pathol. 2014;27:1479–88.

Rossi G, Cavazza A, Sturm N, Migaldi M, Facciolongo N, Longo L, et al. Pulmonary carcinomas with pleomorphic, sarcomatoid, or sarcomatous elements: a clinicopathologic and immunohistochemical study of 75 cases. Am J Surg Pathol. 2003;27:311–24.

Rossi G, Mengoli MC, Cavazza A, Nicoli D, Barbareschi M, Cantaloni C, et al. Large cell carcinoma of the lung: clinically oriented classification integrating immunohistochemistry and molecular biology. Virchows Arch. 2014;464:61–8.

Terry J, Leung S, Laskin J, Leslie O, Gown AM, Ionescu DN. Optimal immunohistochemical markers for distinguishing lung adenocarcinomas from squamous cell carcinomas in small tumor samples. Am J Surg Pathol. 2010;34:1805–11.

Travis WD. Update on small cell carcinoma and its differentiation from squamous cell carcinoma and other non-small cell carcinomas. Mod Pathol. 2012;25(Suppl 1):S18–30.

Travis WD, Linnoila RI, Tsokos MG, Hitchcock CL, Cutler GB Jr, Nieman L, et al. Neuroendocrine tumors of the lung with proposed criteria for large-cell neuroendocrine carcinoma. An ultrastructural, immunohistochemical, and flow cytometric study of 35 cases. Am J Surg Pathol. 1991;15:529–53.

Travis WD, Rush W, Flieder DB, Falk R, Fleming MV, Gal AA, et al. Survival analysis of 200 pulmonary neuroendocrine tumors with clarification of criteria for atypical carcinoid and its separation from typical carcinoid. Am J Surg Pathol. 1998;22:934–44.

Travis WD, Brambilla E, Noguchi M, Nicholson AG, Geisinger KR, Yatabe Y, et al. International Association for the Study of Lung Cancer/American Thoracic Society/European Respiratory Society international multidisciplinary classification of lung adenocarcinoma. J Thorac Oncol. 2011;6:244–85.

Travis WD, Brambilla E, Noguchi M, Nicholson AG, Geisinger K, Yatabe Y, et al. Diagnosis of lung cancer in small biopsies and cytology: implications of the 2011 International Association for the Study of Lung Cancer/American Thoracic Society/European Respiratory Society classification. Arch Pathol Lab Med. 2013a;137:668–84.

Travis WD, Brambilla E, Noguchi M, Nicholson AG, Geisinger K, Yatabe Y, et al. Diagnosis of lung adenocarcinoma in resected specimens: implications of the 2011 International Association for the Study of Lung Cancer/American Thoracic Society/European Respiratory Society classification. Arch Pathol Lab Med. 2013b;137:685–705.

Yoshizawa A, Sumiyoshi S, Sonobe M, Kobayashi M, Fujimoto M, Kawakami F, et al. Validation of the IASLC/ATS/ERS lung adenocarcinoma classification for prognosis and association with EGFR and KRAS gene mutations: analysis of 440 Japanese patients. J Thorac Oncol. 2013;8:52–61.